NATIONAL ADVISORY COMMITTEE FOR AERONAUTICS

TECHNICAL NOTE 3076

LIFT AND MOMENT COEFFICIENTS EXPANDED TO THE SEVENTH POWER OF FREQUENCY FOR OSCILLATING RECTANGULAR WINGS IN SUPERSONIC FLOW AND APPLIED TO A SPECIFIC FLUTTER PROBLEM

By Herbert C. Nelson, Ruby A. Rainey, and Charles E. Watkins

Langley Aeronautical Laboratory
Langley Field, Va.

Washington
April 1954

NATIONAL ADVISORY COMMITTEE FOR AERONAUTIC

TECHNICAL NOTE 3076

LIFT AND MOMENT COEFFICIENTS EXPANDED TO THE SEVENTH POWER OF FREQUENCY FOR OSCILLATING RECTANGULAR WINGS IN SUPERSONIC FLOW AND APPLIED TO A SPECIFIC FLUTTER PROBLEM

By Herbert C. Nelson, Ruby A. Rainey, and Charles E. Watkins

SUMMARY

Linearized theory for compressible unsteady flow is used to derive the velocity potential and lift and moment coefficients in the form of power series in terms of the frequency of oscillation for a harmonically oscillating rectangular wing moving at a constant supersonic speed. Closed expressions for the velocity potential and lift and moment coefficients associated with pitching and translation are given to the seventh power of the frequency. These expressions extend the range of usefulness of NACA Report 1028 in which similar expressions were derived to the third power of the frequency of oscillation. For example, at a Mach number of 10/9 the expansion of the potential to the third power is an accurate representation of the potential for values of the reduced frequency only up to about 0.08; whereas the expansion of the potential to the seventh power is an accurate representation for values of the reduced frequency up to about 0.2, a value of this parameter large enough to cover most rectangular-wing flutter cases likely to occur at this Mach number.

The section and total lift and moment coefficients are discussed with the aid of several figures. In addition, flutter speeds obtained in the Mach number range from 10/9 to 10/6 for a rectangular wing of aspect ratio 4.53 by using section coefficients derived on the basis of three-dimensional flow are compared with flutter speeds for this wing obtained by using coefficients derived on the basis of two-dimensional flow.

INTRODUCTION

A method for obtaining the air forces and moments acting on harmonically oscillating rectangular wings in supersonic flow is given in reference 1. This method is based on the expansion of the velocity potential

in powers of the frequency of oscillation and is applied to harmonically translating and pitching rectangular wings to obtain expressions for the associated forces and moments involving the frequency to the third power.

In the expansion of the velocity potential, the frequency of oscillation and Mach number enter the results in a combined form such that the range of frequency for which the expansion to a given power represents an acceptable approximation to the actual potential decreases as the Mach number decreases toward unity. As a result, the force and moment expressions of reference 1 apply to a sufficiently broad frequency range for most flutter studies only if the stream Mach number is greater than about 1.5. In order to obtain results that cover a larger part of the transonic range, that is, results that apply over a wider frequency range at Mach numbers nearer unity, the present paper extends to the seventh power of the frequency the expressions of reference 1 for velocity potential, section force and moment coefficients, and total force and moment coefficients. This extension results in a coverage of frequency that is generally sufficient at Mach numbers as low as about 1.1. It also, of course, increases the frequency range covered by the approximate theory at all supersonic Mach numbers.

Although the method of reference 1 furnishes a straightforward approach for making this extension, the present paper employs a more concise method based on the velocity potential for a semi-infinite wing, developed in reference 2. In this reference Stewartson makes use of the Laplace transformation to obtain the potential in the form of a definite integral. The integrand of this integral expanded in powers of the frequency and integrated term by term can be made to yield results that are identical in form with those obtained by the method of reference 1. For the sake of completeness Stewartson's derivation of the velocity potential for the semi-infinite wing is reconsidered herein.

For illustration the extended section coefficients are used to calculate flutter characteristics for a rectangular wing of aspect ratio 4.53 at several Mach numbers in the low supersonic speed range. These results are compared with calculations made by using two-dimensional aerodynamic coefficients, obtained from reference 3.

SYMBOLS

A	aspect ratio
b	one-half chord
c	speed of sound in undisturbed medium

c_l	section lift coefficient
C_L	total lift coefficient
c_m	section pitching-moment coefficient about axis of rotation x_o
C_m	total pitching-moment coefficient about axis of rotation x_o
$F_n(x,y)$	functions defined after equation (17)
$\bar{F}_n = F_n(1,y)$	
h	vertical displacement of axis of rotation x_o, positive downward
h_o	amplitude of vertical displacement
$\dot{h},\dot{\alpha}$	time derivatives of h and α, respectively
$J_0(\sigma)$	Bessel function of zero order (first kind)
k	reduced frequency, $\omega b/V$
L_i,M_i	components of section force and moment coefficients, respectively, defined in equations (29) to (32); $i = 1, 2, 3$, and 4
$\bar{L}_i,\bar{M}_i$	components of total force and moment coefficients, respectively, defined in equations (37) and (38); $i = 1, 2, 3$, and 4
M	Mach number, V/c
M_α	aerodynamic section moment on wing about axis of rotation x_o, positive leading edge up
$\bar{M}_\alpha$	total aerodynamic moment on wing about axis of rotation x_o, positive leading edge up
Δp	local pressure difference
P	aerodynamic section normal force, positive downward

$\overline{P}$ total aerodynamic force on wing, positive downward

r_α nondimensional radius of gyration of wing section about elastic axis, $\sqrt{I_\alpha/mb^2}$ where I_α is mass moment of inertia per unit span about elastic axis and m is mass of wing per unit span

s one-half span of wing

t time

V velocity

$w(x',y_m',t)$ vertical velocity at surface of wing along chordwise section $y' = y_m'$

x_α location of center of gravity of wing measured from elastic axis (see ref. 3)

x_o abscissa of axis of rotation of wing (elastic axis)

x,y,z nondimensional rectangular coordinates attached to wing moving in negative x-direction, referred to wing chord $2b$

$x' = 2bx$

$y' = 2by$

$z' = 2bz$

Z_h first bending mode shape of wing

Z_m vertical displacement of any chordwise section of wing

Z_α first torsion mode shape of wing

α angle of attack, positive leading edge up

α_h effective angle of attack due to vertical translation, $\dot{h}/V$

α_o amplitude of angle of attack α

$\beta = \sqrt{M^2 - 1}$

$\zeta = 2y/A$

θ_h phase angle between section lift due to h and velocity $\dot{h}$

θ_α phase angle between section lift due to α and position α

θ_{hm} phase angle between section moment due to h and velocity $\dot{h}$

$\theta_{\alpha m}$ phase angle between section moment due to α and position α

θ_A phase angle between total lift due to α and position α

θ_{AM} phase angle between total moment due to α and position α

κ density parameter, $\pi\rho b^2/m$

ρ density in undisturbed medium

ϕ disturbance-velocity potential

ω frequency of oscillation

ω_h first bending frequency of wing

ω_α first torsion frequency of wing

$\bar{\omega} = 2kM^2/\beta^2$

ANALYSIS

Velocity Potentials for Harmonically Oscillating Rectangular Wings

As a first step in the analysis, an integral expression is developed for the velocity potential for a harmonically oscillating semi-infinite rectangular wing (fig. 1). As mentioned in the introduction this expression is given in reference 2 and is redeveloped herein for the sake of completeness. From the expression for the semi-infinite wing, the potentials for the various regions (see fig. 2(a)) of a finite rectangular

wing are obtained either directly or by appropriate modifications. The analysis for the finite wing, like that of reference 1, is restricted to the condition that the Mach line from the foremost point of one wing tip does not intersect the opposite tip ahead of the trailing edge.

Velocity potential for semi-infinite rectangular wing.- Consider a thin, flat, semi-infinite, rectangular wing moving at a constant supersonic speed in a chordwise direction normal to its leading edge as shown in figure 1. The differential equation satisfied by the disturbance-velocity potential for the wing (when referred to a rectangular coordinate system x',y',z' moving uniformly in the negative x'-direction with the $x'y'$-plane coincident with the mean position of the wing) is

$$\frac{1}{c^2}\left(\frac{\partial}{\partial t} + V\frac{\partial}{\partial x'}\right)^2 \phi = \frac{\partial^2\phi}{\partial x'^2} + \frac{\partial^2\phi}{\partial y'^2} + \frac{\partial^2\phi}{\partial z'^2} \tag{1}$$

where $x' = 2bx$, $y' = 2by$, $z' = 2bz$, $2b$ is the wing chord, and c is the speed of sound in the undisturbed medium. The boundary condition of tangential flow at the surface of the wing, in accordance with small-disturbance linearized theory, can be expressed as

$$\left(\frac{\partial\phi}{\partial z'}\right)_{z'\to\pm 0} = w(x',y_m',t) = V\frac{\partial Z_m}{\partial x'} + \frac{\partial Z_m}{\partial t} \tag{2}$$

where Z_m is the vertical displacement of the ordinates of the surface of any chordwise section of the wing such as $y' = y_m'$ in figure 2. The wing is assumed to be executing simple harmonic motion with respect to time t, so that t enters only in the exponential $\exp(i\omega t)$, where ω is the frequency of oscillation. Equation (1) thus becomes

$$\frac{\partial^2\psi}{\partial y'^2} + \frac{\partial^2\psi}{\partial z'^2} = \beta^2\frac{\partial^2\psi}{\partial x'^2} + \frac{2i\omega M}{c}\frac{\partial\psi}{\partial x'} - \frac{\omega^2}{c^2}\psi \tag{3}$$

where the disturbance-velocity potential ϕ is related to ψ by

$$\phi(x',y',z',t) = \psi(x',y',z')e^{i\omega t}$$

For the case of the semi-infinite wing having identical motion in every chordwise section the boundary conditions that equation (3) must satisfy are:

$$\left(\frac{\partial \psi}{\partial z'}\right)_{z'=\pm 0} = w(x') \qquad (x', y' \geq 0) \qquad (4)$$

$$i\omega\psi + V\frac{\partial \psi}{\partial x'} = 0 \qquad (y' < 0) \qquad (5)$$

$$\psi = 0 \qquad (x' < 0) \qquad (6)$$

$$\psi \longrightarrow 0 \qquad (z' \longrightarrow \pm\infty) \qquad (7)$$

Equation (4) is derived from equation (2) and implies that the normal-velocity distribution on the wing is given; equation (5) is the condition that the pressure be zero off the tip of the wing; equation (6) is the condition that no disturbances be propagated forward of the wing; and equation (7) is a condition on the behavior at infinity (the manner of approaching zero is associated with the radiation condition of Sommerfeld). Equations (3) to (7) constitute the boundary-value problem for the velocity potential ϕ.

Applying the Laplace transform

$$\overline{\psi}(s,y',z') = \int_0^\infty e^{-sx'}\psi(x',y',z')dx'$$

to equations (3) to (7) yields the transformed boundary-value problem in the form

$$\frac{\partial^2\overline{\psi}}{\partial y'^2} + \frac{\partial^2\overline{\psi}}{\partial z'^2} = \left(\beta^2 s^2 + i\,\frac{2\alpha M}{c}\,s - \frac{\omega^2}{c^2}\right)\overline{\psi} \equiv \mu^2\overline{\psi} \qquad (8)$$

$$\left(\frac{\partial\overline{\psi}}{\partial z'}\right)_{z'=\pm 0} = w(s) \qquad (y' \geq 0) \qquad (9)$$

$$\bar{\psi} = 0 \qquad (y' < 0) \tag{10}$$

$$\bar{\psi} \longrightarrow 0 \qquad (z' \longrightarrow \pm\infty) \tag{11}$$

The problem in this form is, as pointed out in reference 2, similar to the problem treated in article 308 of reference 4. By applying the method of reference 4 to the present problem, it can be shown that the value for $\bar{\psi}$ at the upper surface of the wing ($z' = +0$) is given by

$$\bar{\psi} = -w(s)\left(\frac{1}{\mu} - \frac{2}{\sqrt{\pi\mu}}\int_{\sqrt{y'}}^{\infty} e^{-\mu\nu^2}d\nu\right) \tag{12}$$

For convenience equation (12) may be rewritten (see, for example, p. 478 of ref. 5) as

$$\bar{\psi} = -w(s)\left(\frac{1}{\mu} - \frac{2}{\pi\mu}\int_{0}^{\pi/2} e^{-\mu y' \sec^2\eta}\, d\eta\right) \tag{13}$$

If use is made of a table of Laplace transforms (for example, pairs 55 and 89 of ref. 6) and the Faltung or convolution theorem, the inverse of the Laplace transform in equation (13) may be written as

$$\psi(x',y',+0) = -\frac{1}{\beta}\int_{0}^{x'} w(x' - \xi')G(\xi',y')d\xi' \tag{14}$$

where

$$G(x',y') = J_0\left(\frac{\omega}{c\beta^2}x'\right)e^{-i\frac{\omega M}{c\beta^2}x'} \qquad (x' < \beta y')$$

$$G(x',y') = \left[J_0\left(\frac{\omega}{c\beta^2}x'\right) - \frac{2}{\pi}\int_{0}^{\sec^{-1}\sqrt{\frac{x'}{\beta y'}}} J_0\left(\frac{\omega}{c\beta^2}\sqrt{x'^2 - \beta^2 y'^2 \sec^4\eta}\right)d\eta\right]e^{-i\frac{\omega M}{c\beta^2}x'} \qquad (x' > \beta y')$$

and $\xi' = 2b\xi$. From equation (14) the velocity potential in terms of the nondimensional coordinates x, ξ, and y becomes

$$\phi(2bx,2by,t) = -\frac{2be^{i\omega t}}{\beta}\int_0^x w\left[\overline{2b}(x - \xi)\right] G(2b\xi,2by)\,d\xi \qquad (15)$$

where

$$G(2bx,2by) = J_0\left(\frac{\overline{\omega}}{M}x\right)e^{-i\overline{\omega}x} \qquad (x < \beta y)$$

$$G(2bx,2by) = \left[J_0\left(\frac{\overline{\omega}}{M}x\right) - \frac{2}{\pi}\int_0^{\sec^{-1}\sqrt{\frac{x}{\beta y}}} J_0\left(\frac{\overline{\omega}}{M}\sqrt{x^2 - \beta^2y^2\sec^4\eta}\right)d\eta\right]e^{-i\overline{\omega}x}$$

$$(x > \beta y)$$

$$\overline{\omega} = \frac{2b\omega M^2}{V\beta^2}$$

Equation (15) is the desired integral expression for the velocity potential for a semi-infinite wing. Note that for $x \leq \beta y$ equation (15) reduces to the potential for a two-dimensional wing (see ref. 3).

An expansion of the integrand of equation (15) in powers of the frequency of oscillation is employed because the indicated integration does not appear to be obtainable in terms of known functions. The result of this expansion is

$$\phi = -\frac{4be^{i\omega t}}{\pi\beta}\int_0^x w\left[2b(x - \xi)\right]\sum_{q=0}^{\infty}(-i\overline{\omega}\xi)^q\sum_{r=0}^{\left[\frac{q}{2}\right]}\frac{1}{(q - 2r)!\,[r!]^2}\left(\frac{1}{2M}\right)^{2r} I_r(\xi,y)\,d\xi \qquad (16)$$

where $\left[q/2\right]$ denotes the integral part of $q/2$ and

$$I_r(x,y) = \frac{\pi}{2} \qquad (x < \beta y)$$

$$I_r(x,y) = \frac{\pi}{2} - \int_0^{\sec^{-1}\sqrt{\frac{x}{\beta y}}} \left(1 - \frac{\beta^2 y^2}{x^2}\sec^4\eta\right)^r d\eta \qquad (x > \beta y)$$

It may be shown by induction that I_r for $x > \beta y$ can be expressed in terms of the functions F_n of reference 1 as follows:

$$I_r = \frac{2r}{x^{2r}} \sum_{m=0}^{r-1} (-1)^m \frac{(r-1)!}{m!(r-m-1)!} x^{2(r-m-1)} F_{2(m+1)}(x,y) \tag{17}$$

where

$$F_n(x,y) = \int_0^x x^{n-1} \sin^{-1}\sqrt{\frac{\beta y}{x}}\, dx$$

Two relations involving F_n that are of particular importance in the next section are

$$\int_0^x x^m F_n(x,y)\,dx = \frac{1}{m+1}\left(x^{m+1}F_n - F_{m+n+1}\right) \tag{18}$$

and

$$F_n(x,y) = \frac{x^n}{n} \sin^{-1}\sqrt{\frac{\beta y}{x}} + \left[\frac{1}{n}\sum_{m=1}^{n} a_m x^{n-m}(\beta y)^{m-1}\right]\sqrt{\beta y(x - \beta y)} \tag{19}$$

where

$$a_1 = \frac{1}{2n-1}$$

$$a_m = \frac{2^{m-1}(n-1)(n-2)\ \ldots\ (n-m+1)}{(2n-1)(2n-3)\ \ldots\ (2n-2m+1)} \qquad (m > 1)$$

Equations (16) to (19) provide the means for obtaining the potential to any desired power of the frequency of oscillation. They are used in the next section to develop expressions to the seventh power of the frequency for the velocity potentials for the various regions of a finite rectangular wing undergoing torsional and vertical translational oscillations. These expressions are extensions of similar expressions developed in reference 1 to the third power of the frequency.

Velocity potentials for finite rectangular wing.- The coordinate system and regions of interest for the finite rectangular wing are shown in figure 2. On the portion of the wing between the Mach cones emanating from the foremost point of each tip (region N in fig. 2(a)) no interaction takes place between the flow on the upper and lower surfaces of the wing. On the portions of the wing within the tip Mach cones (regions T_1, T_2, and T_3 in fig. 2(a)) interaction does take place between the flow on the upper and lower surfaces. The velocity potential at a point in one of these regions is designated by ϕ_N, ϕ_{T_1}, ϕ_{T_2}, or ϕ_{T_3} according to the region that contains the point.

For the particular case of the wing independently performing small sinusoidal torsional oscillations of amplitude α_o about some spanwise axis x_o and small sinusoidal vertical translations of amplitude h_o, the equation for Z_m is (see fig. 2(b))

$$Z_m = e^{i\omega t}\left[2b\alpha_o(x - x_o) + h_o\right] = 2b\alpha(x - x_o) + h \qquad (20)$$

Substituting this expression for Z_m into equation (2) gives

$$w(2bx,t) = V\alpha + 2b\dot{\alpha}(x - x_o) + \dot{h} \qquad (21)$$

Equation (21) complies with the restriction inherent in the development of equation (15), namely, that the wing have identical motion in every chordwise section.

The velocity potential for region T_1 for the wing motion represented by equation (20) is obtained directly from equation (16). Putting the expression for $w(2bx,t)$ given by equation (21) into equation (16), retaining only terms in the expansion up to the seventh power of $\overline{\omega}$, inserting the appropriate values of I_r obtained from equation (17),

and performing the necessary integrations with the aid of equation (18) yields the following form for the velocity potential in region T_1:

$$\phi_{T_1} = -\frac{2b}{\beta}\left\{(\dot{h} + V\alpha)\lambda_1(x,y) + 2b\dot{\alpha}\left[\lambda_2(x,y) - x_o\lambda_1(x,y)\right]\right\} \tag{22}$$

where

$$\lambda_1(x,y) = \frac{2}{\pi}\left\{F_1 - i\bar{\omega}F_2 - \frac{\bar{\omega}^2}{2M^2}\left(xF_2 + \beta^2F_3\right) + \frac{i\bar{\omega}^3}{12M^2}\left[3x^2F_2 + (2\beta^2 - 1)F_4\right] + \right.$$

$$\frac{\bar{\omega}^4}{48M^4}\left[x^3\left(4\beta^2 + 5\right)F_2 - 3xF_4 + 2\beta^4F_5\right] - \frac{i\bar{\omega}^5}{960M^4}\left[5x^4\left(4\beta^2 + 7\right)F_2 -\right.$$

$$30x^2F_4 + \left(8\beta^4 - 4\beta^2 + 3\right)F_6\left.\right] - \frac{\bar{\omega}^6}{5760M^6}\left[3x^5\left(8\beta^4 + 28\beta^2 + 21\right)F_2 -\right.$$

$$10x^3\left(6\beta^2 + 7\right)F_4 + 15xF_6 + 8\beta^6F_7\left.\right] + \frac{i\bar{\omega}^7}{80640M^6}\left[7x^6\left(8\beta^4 +\right.\right.$$

$$\left.36\beta^2 + 33\right)F_2 - 105x^4\left(2\beta^2 + 3\right)F_4 + 105x^2F_6 +$$

$$\left.\left(16\beta^6 - 8\beta^4 + 6\beta^2 - 5\right)F_8\right]\Bigg\}$$

$$\lambda_2(x,y) = \int_0^x \lambda_1(x,y)\,dx$$

The integrations required to obtain the function λ_2 may be readily performed with the aid of equation (18). The integrated values of F_n (from eq. (19)) needed in equation (22) are listed in appendix A.

Use is now made of the potential ϕ_{T_1}, equation (22), to obtain the potentials for regions N, T_2, and T_3. The potential ϕ_N is obtained

from ϕ_{T_1} by substituting $y = x/\beta$ in the functions λ_1 and λ_2 in equation (22), in which case F_n becomes

$$F_n = \frac{\pi}{2}\frac{x^n}{n}$$

and the velocity potential ϕ_N is given by

$$\phi_N = -\frac{2b}{\beta}\left\{(\dot{h} + V\alpha)f_1(x) + 2b\dot{\alpha}\left[f_2(x) - x_o f_1(x)\right]\right\} \tag{23}$$

where

$$f_1(x) = x - i\bar{\omega}\frac{x^2}{2} - \frac{\bar{\omega}^2}{4M^2}\left(2\beta^2 + 3\right)\frac{x^3}{3} + \frac{i\bar{\omega}^3}{12M^2}\left(2\beta^2 + 5\right)\frac{x^4}{4} + \frac{\bar{\omega}^4}{192M^4}\left(8\beta^4 +$$

$$40\beta^2 + 35\right)\frac{x^5}{5} - \frac{i\bar{\omega}^5}{960M^4}\left(8\beta^4 + 56\beta^2 + 63\right)\frac{x^6}{6} - \frac{\bar{\omega}^6}{11520M^6}\left(16\beta^6 + 168\beta^4 +$$

$$378\beta^2 + 231\right)\frac{x^7}{7} + \frac{i\bar{\omega}^7}{80640M^6}\left(16\beta^6 + 216\beta^4 + 594\beta^2 + 429\right)\frac{x^8}{8}$$

$$f_2(x) = \int_0^x f_1(x)dx$$

Note that because of the two-dimensional character of the problem in region N the spanwise variable y is not contained in ϕ_N. Equation (23) can also be obtained by expanding to the seventh power of $\bar{\omega}$ the velocity potential for the two-dimensional wing given in reference 3. The potential ϕ_{T_2} is obtained from ϕ_{T_1} by replacing y in the functions λ_1 and λ_2 in equation (22) by A - y, where $A = 2s/2b$ is the aspect ratio. The potential in region T_3 (this region exists if $1 < A\beta < 2$) is a simple superposition of the potentials for regions N, T_1, and T_2, as indicated in reference 1, and may be written as

$$\phi_{T_3} = \phi_{T_1} + \phi_{T_2} - \phi_N \tag{24}$$

Forces and Moments

Section forces and moments.- The expanded velocity potentials for the finite wing are now used to obtain expressions for the section forces and moments at any spanwise station of the wing. Since the distribution over the entire wing is symmetrical with respect to the midspan section, only expressions for the forces and moments at any station of the one-half span adjacent to the origin (see fig. 2) need be considered.

The local pressure difference between the upper and lower surfaces of the wing may be written as

$$\Delta p = -2\rho\left(\frac{V}{2b}\frac{\partial \phi}{\partial x} + i\omega\phi\right) \tag{25}$$

The section force, positive downward, is therefore

$$P = -2b\int_0^1 \Delta p \, dx \tag{26}$$

and the section moment, positive leading edge up, about the arbitrary axis of rotation $x = x_o$ is

$$M_\alpha = -4b^2\int_0^1 (x - x_o)\Delta p \, dx \tag{27}$$

Under the previously mentioned restriction that the Mach line from one tip not intersect the opposite tip ahead of the trailing edge, equations (26) and (27) must be evaluated for the two cases that can arise (see fig. 3). These cases are: (1) The Mach lines from the tips do not intersect on the wing ($A\beta > 2$) and (2) the Mach lines intersect on the wing but the Mach line from one tip does not intersect the opposite tip ahead of the trailing edge ($1 \leq A\beta \leq 2$). Only the final forms of the section forces and moments are given. These forms are calculated by deriving the pressure difference for the different regions from the appropriate velocity potentials, making use of figure 3 to determine the limits of integration for the regions involved, and using the relation given in equation (18) to perform the integrations involving the functions F_n; the results can be written as

$$\left.\begin{aligned} P &= -4\rho bV^2k^2e^{i\omega t}\left[\frac{h_o}{b}\left(L_1 + iL_2\right) + \alpha_o\left(L_3 + iL_4\right)\right] \\ M_\alpha &= -4\rho b^2V^2k^2e^{i\omega t}\left[\frac{h_o}{b}\left(M_1 + iM_2\right) + \alpha_o\left(M_3 + iM_4\right)\right] \end{aligned}\right\} \tag{28}$$

The quantities L_i (i = 1, 2, 3, and 4) and M_i (i = 1, 2, 3, and 4) are the components of the section force and section moment coefficients, respectively. The reduced frequency k is related to ω and $\bar{\omega}$ by the relations

$$k = \frac{b\omega}{V} = \frac{\beta^2}{2M^2}\bar{\omega}$$

In order to obtain self-consistent expressions for the forces and moments, the terms of the velocity potentials associated with h and α are expanded to the seventh power of $\bar{\omega}$ and the terms associated with $\dot{\alpha}$ are expanded to the sixth power. As a result, the coefficients in equations (28) are as follows:

Case 1(see fig. 3(a)): For any section between the tip and the point where the Mach line intersects the trailing edge, or where $0 < y < 1/\beta$,

$$L_1 = \frac{1}{\pi\beta^3}\left\{4\left[-\beta^2\bar{\bar{F}}_1 + \left(2\beta^2 + 1\right)\bar{\bar{F}}_2\right] - \frac{1}{3}\left[3\bar{\bar{F}}_2 - 6\beta^4\bar{\bar{F}}_3 + \left(8\beta^4 + 4\beta^2 - 1\right)\bar{\bar{F}}_4\right]\left(\frac{\bar{\omega}}{M}\right)^2 + \right.$$

$$\frac{1}{240}\left[5\left(6\beta^2 + 7\right)\bar{\bar{F}}_2 - 30\bar{\bar{F}}_4 - 40\beta^6\bar{\bar{F}}_5 + 3\left(16\beta^6 + 8\beta^4 - 2\beta^2 + 1\right)\bar{\bar{F}}_6\right]\left(\frac{\bar{\omega}}{M}\right)^4 -$$

$$\frac{1}{20160}\left[7\left(16\beta^4 + 48\beta^2 + 33\right)\bar{\bar{F}}_2 - 35\left(8\beta^2 + 9\right)\bar{\bar{F}}_4 + 105\bar{\bar{F}}_6 - 112\beta^8\bar{\bar{F}}_7 + \right.$$

$$\left.\left.\left(128\beta^8 + 64\beta^6 - 16\beta^4 + 8\beta^2 - 5\right)\bar{\bar{F}}_8\right]\left(\frac{\bar{\omega}}{M}\right)^6\right\} \tag{29a}$$

$$L_2 = \frac{1}{\pi\beta k}\left\{2\bar{\bar{F}}_1 + \left[\left(2\beta^2 - 1\right)\bar{\bar{F}}_2 - 3\beta^2\bar{\bar{F}}_3\right]\left(\frac{\varpi}{M}\right)^2 + \frac{1}{24}\left[5\bar{\bar{F}}_2 - \left(8\beta^4 - 4\beta^2 + 3\right)\bar{\bar{F}}_4 + 10\beta^4\bar{\bar{F}}_5\right]\left(\frac{\varpi}{M}\right)^4 - \frac{1}{2880}\left[21\left(2\beta^2 + 3\right)\bar{\bar{F}}_2 - 70\bar{\bar{F}}_4 - 3\left(16\beta^6 - 8\beta^4 + 6\beta^2 - 5\right)\bar{\bar{F}}_6 + 56\beta^6\bar{\bar{F}}_7\right]\left(\frac{\varpi}{M}\right)^6\right\} \tag{29b}$$

$$L_3 = \frac{1}{\pi\beta M^2k^2}\left\{2\left(\beta^2 + 1\right)\bar{\bar{F}}_1 - \left[\beta^4\bar{\bar{F}}_1 - \left(6\beta^4 + 3\beta^2 - 1\right)\bar{\bar{F}}_2 + \beta^2\left(6\beta^2 + 5\right)\bar{\bar{F}}_3\right]\left(\frac{\varpi}{M}\right)^2 + \frac{1}{24}\left[\left(\beta^2 + 5\right)\bar{\bar{F}}_2 + 12\beta^6\bar{\bar{F}}_3 - \left(40\beta^6 + 20\beta^4 - 5\beta^2 + 3\right)\bar{\bar{F}}_4 + 2\beta^4\left(15\beta^2 + 13\right)\bar{\bar{F}}_5\right]\left(\frac{\varpi}{M}\right)^4 - \frac{1}{2880}\left[3\left(2\beta^4 + 21\beta^2 + 21\right)\bar{\bar{F}}_2 - 10\left(\beta^2 + 7\right)\bar{\bar{F}}_4 + 120\beta^8\bar{\bar{F}}_5 - 3\left(112\beta^8 + 56\beta^6 - 14\beta^4 + 7\beta^2 - 5\right)\bar{\bar{F}}_6 + 8\beta^6\left(28\beta^2 + 25\right)\bar{\bar{F}}_7\right]\left(\frac{\varpi}{M}\right)^6\right\} - 2x_oL_1 \tag{29c}$$

$$L_4 = \frac{1}{\pi\beta^3k}\left\{4\left[2\beta^2\bar{\bar{F}}_1 - \left(3\beta^2 + 1\right)\bar{\bar{F}}_2\right] + \frac{1}{3}\left[3\left(2\beta^4 - \beta^2 + 1\right)\bar{\bar{F}}_2 - 24\beta^4\bar{\bar{F}}_3 + \left(20\beta^4 + 7\beta^2 - 1\right)\bar{\bar{F}}_4\right]\left(\frac{\varpi}{M}\right)^2 - \frac{1}{240}\left[5\left(\beta^2 + 7\right)\bar{\bar{F}}_2 + 10\left(8\beta^6 - 4\beta^4 + 3\beta^2 - 3\right)\bar{\bar{F}}_4 - 240\beta^6\bar{\bar{F}}_5 + \left(168\beta^6 + 64\beta^4 - 11\beta^2 + 3\right)\bar{\bar{F}}_6\right]\left(\frac{\varpi}{M}\right)^4 + \frac{1}{20160}\left[7\left(2\beta^4 + 27\beta^2 + 33\right)\bar{\bar{F}}_2 - 35\left(\beta^2 + 9\right)\bar{\bar{F}}_4 + 21\left(16\beta^8 - 8\beta^6 + 6\beta^4 - 5\beta^2 + 5\right)\bar{\bar{F}}_6 - 896\beta^8\bar{\bar{F}}_7 + \left(576\beta^8 + 232\beta^6 - 44\beta^4 + 15\beta^2 - 5\right)\bar{\bar{F}}_8\right]\left(\frac{\varpi}{M}\right)^6\right\} - 2x_oL_2 \tag{29d}$$

$$M_1 = \frac{1}{\pi\beta^3}\left\{4\left[-\beta^2\bar{\bar{F}}_1 + \left(3\beta^2 + 2\right)\bar{\bar{F}}_3\right] - \frac{2}{3}\left[2\bar{\bar{F}}_2 - 3\beta^4\bar{\bar{F}}_3 + \beta^2\left(5\beta^2 + 4\right)\bar{\bar{F}}_5\right]\left(\frac{\varpi}{M}\right)^2 + \right.$$

$$\frac{1}{30}\left[\left(6\beta^2 + 7\right)\bar{\bar{F}}_2 - 5\bar{\bar{F}}_4 - 5\beta^6\bar{\bar{F}}_5 + \beta^4\left(7\beta^2 + 6\right)\bar{\bar{F}}_7\right]\left(\frac{\varpi}{M}\right)^4 -$$

$$\frac{1}{5040}\left[3\left(16\beta^4 + 48\beta^2 + 33\right)\bar{\bar{F}}_2 - 14\left(8\beta^2 + 9\right)\bar{\bar{F}}_4 + 35\bar{\bar{F}}_6 - \right.$$

$$\left.\left. 28\beta^8\bar{\bar{F}}_7 + 4\beta^6\left(9\beta^2 + 8\right)\bar{\bar{F}}_9\right]\left(\frac{\varpi}{M}\right)^6\right\} - 2x_oL_1 \qquad (30a)$$

$$M_2 = \frac{1}{\pi\beta k}\left\{4\bar{\bar{F}}_2 - \left[-\left(2\beta^2 - 1\right)\bar{\bar{F}}_2 + \left(4\beta^2 + 1\right)\bar{\bar{F}}_4\right]\left(\frac{\varpi}{M}\right)^2 + \frac{1}{48}\left[15\bar{\bar{F}}_2 - 2\left(8\beta^4 - \right.\right.\right.$$

$$\left.\left.\left. 4\beta^2 + 3\right)\bar{\bar{F}}_4 + \left(24\beta^4 + 8\beta^2 - 1\right)\bar{\bar{F}}_6\right]\left(\frac{\varpi}{M}\right)^4 - \frac{1}{2880}\left[35\left(2\beta^2 + 3\right)\bar{\bar{F}}_2 - 105\bar{\bar{F}}_4 - \right.\right.$$

$$\left.\left. 3\left(16\beta^6 - 8\beta^4 + 6\beta^2 - 5\right)\bar{\bar{F}}_6 + \left(64\beta^6 + 24\beta^4 - 4\beta^2 + 1\right)\bar{\bar{F}}_8\right]\left(\frac{\varpi}{M}\right)^6\right\} - 2x_oL_2 \qquad (30b)$$

$$M_3 = \frac{1}{\pi\beta M^2k^2}\left\{4\left(\beta^2 + 1\right)\bar{\bar{F}}_2 - \frac{1}{3}\left[4\beta^4\bar{\bar{F}}_1 - 3\left(6\beta^4 + 3\beta^2 - 1\right)\bar{\bar{F}}_2 + \left(20\beta^4 + \right.\right.\right.$$

$$\left.\left.\left. 21\beta^2 + 3\right)\bar{\bar{F}}_4\right]\left(\frac{\varpi}{M}\right)^2 + \frac{1}{48}\left[3\left(\beta^2 + 5\right)\bar{\bar{F}}_2 + 32\beta^6\bar{\bar{F}}_3 - 2\left(40\beta^6 + 20\beta^4 - \right.\right.\right.$$

$$\left.\left.\left. 5\beta^2 + 3\right)\bar{\bar{F}}_4 + \left(56\beta^6 + 64\beta^4 + 11\beta^2 - 1\right)\bar{\bar{F}}_6\right]\left(\frac{\varpi}{M}\right)^4 - \frac{1}{2880}\left[5\left(2\beta^4 + \right.\right.\right.$$

$$\left.\left.\left. 21\beta^2 + 21\right)\bar{\bar{F}}_2 - 15\left(\beta^2 + 7\right)\bar{\bar{F}}_4 + 160\beta^8\bar{\bar{F}}_5 - 3\left(112\beta^8 + 56\beta^6 - \right.\right.\right.$$

(Equation continued on next page)

$$14\beta^4 + 7\beta^2 - 5)\bar{\bar{F}}_6 + \left(192\beta^8 + 232\beta^6 + 44\beta^4 - 5\beta^2 + 1\right)\bar{\bar{F}}_8\Big]\left(\frac{\varpi}{M}\right)^6\Bigg\} -$$

$$2x_o\left(M_1 + L_3 + 2x_oL_1\right) \tag{30c}$$

$$M_4 = \frac{1}{\pi\beta^3 k}\Bigg\{-8\Big[-\beta^2\bar{\bar{F}}_1 + \left(2\beta^2 + 1\right)\bar{\bar{F}}_3\Big] + \frac{4}{3}\Big[\left(2\beta^4 - \beta^2 + 1\right)\bar{\bar{F}}_2 - 6\beta^4\bar{\bar{F}}_3 +$$

$$\beta^2\left(5\beta^2 + 3\right)\bar{\bar{F}}_5\Big]\left(\frac{\varpi}{M}\right)^2 - \frac{1}{90}\Big[3\left(\beta^2 + 7\right)\bar{\bar{F}}_2 + 5\left(8\beta^6 - 4\beta^4 + 3\beta^2 - 3\right)\bar{\bar{F}}_4 -$$

$$90\beta^6\bar{\bar{F}}_5 + 2\beta^4\left(28\beta^2 + 19\right)\bar{\bar{F}}_7\Big]\left(\frac{\varpi}{M}\right)^4 + \frac{1}{5040}\Big[3\left(2\beta^4 + 27\beta^2 + 33\right)\bar{\bar{F}}_2 -$$

$$14\left(\beta^2 + 9\right)\bar{\bar{F}}_4 + 7\left(16\beta^8 - 8\beta^6 + 6\beta^4 - 5\beta^2 + 5\right)\bar{\bar{F}}_6 - 224\beta^8\bar{\bar{F}}_7 +$$

$$8\beta^6\left(15\beta^2 + 11\right)\bar{\bar{F}}_9\Big]\left(\frac{\varpi}{M}\right)^6\Bigg\} - 2x_o\left(M_2 + L_4 + 2x_oL_2\right) \tag{30d}$$

where $\bar{\bar{F}}_n$ $(n = 1, 2, \ldots 9)$, given in appendix A, is F_n evaluated at $x = 1$. For any section between the point where the Mach line intersects the trailing edge and the midspan, or where $1/\beta < y \leq A/2$,

$$L_1 = \frac{1}{\beta^3}\Bigg[1 - \frac{4\beta^2 + 5}{24}\left(\frac{\varpi}{M}\right)^2 + \frac{8\beta^4 + 28\beta^2 + 21}{960}\left(\frac{\varpi}{M}\right)^4 -$$

$$\frac{64\beta^6 + 432\beta^4 + 792\beta^2 + 429}{322560}\left(\frac{\varpi}{M}\right)^6\Bigg] \tag{31a}$$

$$L_2 = \frac{1}{\beta k}\Bigg[1 - \frac{1}{4}\left(\frac{\varpi}{M}\right)^2 + \frac{4\beta^2 + 7}{192}\left(\frac{\varpi}{M}\right)^4 - \frac{8\beta^4 + 36\beta^2 + 33}{11520}\left(\frac{\varpi}{M}\right)^6\Bigg] \tag{31b}$$

$$L_3 = \frac{1}{\beta M^2 k^2}\left[\beta^2 + 1 - \frac{\beta^2 + 3}{12}\left(\frac{\varpi}{M}\right)^2 + \frac{4\beta^4 + 35\beta^2 + 35}{960}\left(\frac{\varpi}{M}\right)^4 - \frac{8\beta^6 + 140\beta^4 + 357\beta^2 + 231}{80640}\left(\frac{\varpi}{M}\right)^6\right] - 2x_o L_1 \tag{31c}$$

$$L_4 = \frac{1}{\beta^3 k}\left[\beta^2 - 1 + \frac{\beta^2 + 5}{24}\left(\frac{\varpi}{M}\right)^2 - \frac{4\beta^4 + 49\beta^2 + 63}{2880}\left(\frac{\varpi}{M}\right)^4 + \frac{8\beta^6 + 180\beta^4 + 561\beta^2 + 429}{322560}\left(\frac{\varpi}{M}\right)^6\right] - 2x_o L_2 \tag{31d}$$

$$M_1 = \frac{1}{\beta^3}\left[\frac{4}{3} - \frac{4\beta^2 + 5}{15}\left(\frac{\varpi}{M}\right)^2 + \frac{8\beta^4 + 28\beta^2 + 21}{560}\left(\frac{\varpi}{M}\right)^4 - \frac{64\beta^6 + 432\beta^4 + 792\beta^2 + 429}{181440}\left(\frac{\varpi}{M}\right)^6\right] - 2x_o L_1 \tag{32a}$$

$$M_2 = \frac{1}{\beta k}\left[1 - \frac{3}{8}\left(\frac{\varpi}{M}\right)^2 + \frac{5(4\beta^2 + 7)}{576}\left(\frac{\varpi}{M}\right)^4 - \frac{7(8\beta^4 + 36\beta^2 + 33)}{46080}\left(\frac{\varpi}{M}\right)^6\right] - 2x_o L_2 \tag{32b}$$

$$M_3 = \frac{1}{\beta M^2 k^2}\left[\beta^2 + 1 - \frac{\beta^2 + 3}{8}\left(\frac{\varpi}{M}\right)^2 + \frac{4\beta^4 + 35\beta^2 + 35}{576}\left(\frac{\varpi}{M}\right)^4 - \frac{8\beta^6 + 140\beta^4 + 357\beta^2 + 231}{46080}\left(\frac{\varpi}{M}\right)^6\right] - 2x_o(M_1 + L_3 + 2x_o L_1) \tag{32c}$$

$$M_4 = \frac{1}{\beta^3 k}\left[\frac{4(\beta^2 - 1)}{3} + \frac{\beta^2 + 5}{15}\left(\frac{\varpi}{M}\right)^2 - \frac{4\beta^4 + 49\beta^2 + 63}{1680}\left(\frac{\varpi}{M}\right)^4 + \frac{8\beta^6 + 180\beta^4 + 561\beta^2 + 429}{181440}\left(\frac{\varpi}{M}\right)^6\right] - 2x_o(M_2 + L_4 + 2x_o L_2) \tag{32d}$$

Case 2 (see fig. 3(b)): For any section between the tip $y' = 0$ and the point where the Mach line from the tip at $y' = 2s$ intersects the trailing edge $\left(\text{or where } 0 < y < A - \frac{1}{\beta}\right)$ the components of the section force and moment coefficients are given by equations (29) and (30), respectively. For any section between the point where the Mach line from the tip at $y' = 2s$ intersects the trailing edge and the midspan $\left(\text{or where } A - \frac{1}{\beta} < y < A/2\right)$ the components of the section force and moment coefficients, respectively, are obtained by first adding to equations (29) and (30) the results of substituting $A - y$ for y in these equations and then substracting equations (31) and (32) from the result. For example, the term of L_1 that does not contain ϖ is given by

$$L_1 = \frac{1}{\pi\beta^3}\left\{-4\beta^2\left[\bar{\bar{F}}_1(y) + \bar{\bar{F}}_1(A - y)\right] + 4(2\beta^2 + 1)\left[\bar{\bar{F}}_2(y) + \bar{\bar{F}}_2(A - y)\right]\right\} - \frac{1}{\beta^3} \tag{33}$$

Total forces and moments.- Expressions for the total forces and moments can be derived by considering only case 1 of the previous section. It can be shown that case 2, although more cumbersome to handle, leads to the same expressions. Therefore the total force, positive downward, may be written as

$$\bar{P} = 4b\int_0^{1/\beta} (P)_{T_1}\, dy + 4b\int_{1/\beta}^{A/2} (P)_N\, dy \tag{34}$$

and the total moment, positive leading edge up, about the axis $x = x_o$ as

$$\bar{M}_\alpha = 4b\int_0^{1/\beta} (M_\alpha)_{T_1}\, dy + 4b\int_{1/\beta}^{A/2} (M_\alpha)_N\, dy \tag{35}$$

In equations (34) and (35) the quantities $(P)_{T_1}$ and $(M_\alpha)_{T_1}$ are the section force and moment, respectively, whose components are given in equations (29) and (30), and $(P)_N$ and $(M_\alpha)_N$ are the section force and moment, respectively, whose components are given in equations (31) and (32).

Upon performing the integrations indicated in equations (34) and (35) with the aid of the relation

$$\int_0^{1/\beta} \bar{\bar{F}}_n \, dy = \frac{2(n+2)}{n(n+1)} \frac{\pi}{8\beta}$$

the results can be written as

$$\left.\begin{aligned} \bar{P} &= -8\rho b^2 V^2 k^2 A e^{i\omega t}\left[\frac{h_o}{b}\left(\bar{L}_1 + i\bar{L}_2\right) + \alpha_o\left(\bar{L}_3 + i\bar{L}_4\right)\right] \\ \bar{M}_\alpha &= -8\rho b^3 V^2 k^2 A e^{i\omega t}\left[\frac{h_o}{b}\left(\bar{M}_1 + i\bar{M}_2\right) + \alpha_o\left(\bar{M}_3 + i\bar{M}_4\right)\right] \end{aligned}\right\} \tag{36}$$

where

$$\bar{L}_1 = \frac{1}{\beta^3}\left\{1 - \frac{4\beta^2 + 5}{24}\left(\frac{\bar{\omega}}{M}\right)^2 + \frac{8\beta^4 + 28\beta^2 + 21}{960}\left(\frac{\bar{\omega}}{M}\right)^4 - \frac{64\beta^6 + 432\beta^4 + 792\beta^2 + 429}{322560}\left(\frac{\bar{\omega}}{M}\right)^6 - \frac{1}{3A\beta}\left[\beta^2 + 2 - \frac{\beta^4 + 8\beta^2 + 8}{20}\left(\frac{\bar{\omega}}{M}\right)^2 + \frac{\beta^6 + 18\beta^4 + 48\beta^2 + 32}{840}\left(\frac{\bar{\omega}}{M}\right)^4 - \frac{\beta^8 + 32\beta^6 + 160\beta^4 + 256\beta^2 + 128}{60480}\left(\frac{\bar{\omega}}{M}\right)^6\right]\right\} \tag{37a}$$

$$\bar{L}_2 = \frac{1}{\beta k}\left\{1 - \frac{1}{4}\left(\frac{\varpi}{M}\right)^2 + \frac{4\beta^2 + 7}{192}\left(\frac{\varpi}{M}\right)^4 - \frac{8\beta^4 + 36\beta^2 + 33}{11520}\left(\frac{\varpi}{M}\right)^6 - \frac{1}{2A\beta}\left[1 - \frac{\beta^2 + 4}{12}\left(\frac{\varpi}{M}\right)^2 + \frac{\beta^4 + 12\beta^2 + 16}{360}\left(\frac{\varpi}{M}\right)^4 - \frac{\beta^6 + 24\beta^4 + 80\beta^2 + 64}{20160}\left(\frac{\varpi}{M}\right)^6\right]\right\} \tag{37b}$$

$$\bar{L}_3 = \frac{1}{\beta M^2 k^2}\left\{\beta^2 + 1 - \frac{\beta^2 + 3}{12}\left(\frac{\varpi}{M}\right)^2 + \frac{4\beta^4 + 35\beta^2 + 35}{960}\left(\frac{\varpi}{M}\right)^4 - \frac{8\beta^6 + 140\beta^4 + 357\beta^2 + 231}{80640}\left(\frac{\varpi}{M}\right)^6 - \frac{1}{2A\beta}\left[\beta^2 + 1 - \frac{3\beta^2 + 4}{12}\left(\frac{\varpi}{M}\right)^2 + \frac{5\beta^4 + 20\beta^2 + 16}{360}\left(\frac{\varpi}{M}\right)^4 - \frac{7\beta^6 + 56\beta^4 + 112\beta^2 + 64}{20160}\left(\frac{\varpi}{M}\right)^6\right]\right\} - 2x_o\bar{L}_1 \tag{37c}$$

$$\bar{L}_4 = \frac{1}{\beta^3 k}\left\{\beta^2 - 1 + \frac{\beta^2 + 5}{24}\left(\frac{\varpi}{M}\right)^2 - \frac{4\beta^4 + 49\beta^2 + 63}{2880}\left(\frac{\varpi}{M}\right)^4 + \frac{8\beta^6 + 180\beta^4 + 561\beta^2 + 429}{322560}\left(\frac{\varpi}{M}\right)^6 + \frac{1}{3A\beta}\left[2 - \frac{\beta^2 + 2}{5}\left(\frac{\varpi}{M}\right)^2 + \frac{3\beta^4 + 16\beta^2 + 16}{420}\left(\frac{\varpi}{M}\right)^4 - \frac{\beta^6 + 10\beta^4 + 24\beta^2 + 16}{7560}\left(\frac{\varpi}{M}\right)^6\right]\right\} - 2x_o\bar{L}_2 \tag{37d}$$

$$\bar{M}_1 = \frac{1}{\beta^3}\left\{\frac{4}{3} - \frac{4\beta^2+5}{15}\left(\frac{\bar{\omega}}{M}\right)^2 + \frac{8\beta^4+28\beta^2+21}{560}\left(\frac{\bar{\omega}}{M}\right)^4 - \frac{64\beta^6+432\beta^4+792\beta^2+429}{181440}\left(\frac{\bar{\omega}}{M}\right)^6 - \frac{1}{2A\beta}\left[\beta^2+2 - \frac{\beta^4+8\beta^2+8}{18}\left(\frac{\bar{\omega}}{M}\right)^2 + \frac{\beta^6+18\beta^4+48\beta^2+32}{720}\left(\frac{\bar{\omega}}{M}\right)^4 - \frac{\beta^8+32\beta^6+160\beta^4+256\beta^2+128}{50400}\left(\frac{\bar{\omega}}{M}\right)^6\right]\right\} - 2x_o\bar{L}_1 \tag{38a}$$

$$\bar{M}_2 = \frac{1}{\beta k}\left\{1 - \frac{3}{8}\left(\frac{\bar{\omega}}{M}\right)^2 + \frac{5\left(4\beta^2+7\right)}{576}\left(\frac{\bar{\omega}}{M}\right)^4 - \frac{7\left(8\beta^4+36\beta^2+33\right)}{46080}\left(\frac{\bar{\omega}}{M}\right)^6 - \frac{1}{3A\beta}\left[2 - \frac{\beta^2+4}{5}\left(\frac{\bar{\omega}}{M}\right)^2 + \frac{\beta^4+12\beta^2+16}{140}\left(\frac{\bar{\omega}}{M}\right)^4 - \frac{\beta^6+24\beta^4+80\beta^2+64}{7560}\left(\frac{\bar{\omega}}{M}\right)^6\right]\right\} - 2x_o\bar{L}_2 \tag{38b}$$

$$\bar{M}_3 = \frac{1}{\beta M^2 k^2}\left\{\beta^2+1 - \frac{\beta^2+3}{8}\left(\frac{\bar{\omega}}{M}\right)^2 + \frac{4\beta^4+35\beta^2+35}{576}\left(\frac{\bar{\omega}}{M}\right)^4 - \frac{8\beta^6+140\beta^4+357\beta^2+231}{46080}\left(\frac{\bar{\omega}}{M}\right)^6 - \frac{1}{3A\beta}\left[2\left(\beta^2+1\right) - \frac{3\beta^2+4}{5}\left(\frac{\bar{\omega}}{M}\right)^2 + \frac{5\beta^4+20\beta^2+16}{140}\left(\frac{\bar{\omega}}{M}\right)^4 - \frac{7\beta^6+56\beta^4+112\beta^2+64}{7560}\left(\frac{\bar{\omega}}{M}\right)^6\right]\right\} - 2x_o\left(\bar{M}_1 + \bar{L}_3 + 2x_o\bar{L}_1\right) \tag{38c}$$

$$\bar{M}_4 = \frac{1}{\beta^3 k}\left\{\frac{4(\beta^2-1)}{3} + \frac{\beta^2+5}{15}\left(\frac{\bar{\omega}}{M}\right)^2 - \frac{4\beta^4+49\beta^2+63}{1680}\left(\frac{\bar{\omega}}{M}\right)^4 + \frac{8\beta^6+180\beta^4+561\beta^2+429}{181440}\left(\frac{\bar{\omega}}{M}\right)^6 + \frac{1}{3A\beta}\left[3 - \frac{\beta^2+2}{3}\left(\frac{\bar{\omega}}{M}\right)^2 + \frac{3\beta^4+16\beta^2+16}{240}\left(\frac{\bar{\omega}}{M}\right)^4 - \frac{\beta^6+10\beta^4+24\beta^2+16}{4200}\left(\frac{\bar{\omega}}{M}\right)^6\right]\right\} - 2x_o\left(\bar{M}_2 + \bar{L}_4 + 2x_o\bar{L}_2\right) \tag{38d}$$

SOME PROPERTIES OF FORCES AND MOMENTS

Examination of some of the properties of the extended section and total forces and moments of the present paper may be of interest. For this purpose consider, first, the conventional coefficients for section lift c_l and section pitching moment c_m that may be obtained from equations (28) as

$$\left.\begin{aligned} c_l &= -\frac{P}{\rho b V^2} = 4\left[-ik(L_1 + iL_2)\alpha_h + k^2(L_3 + iL_4)\alpha\right] \\ c_m &= \frac{M_\alpha}{2\rho b^2 V^2} = -2\left[-ik(M_1 + iM_2)\alpha_h + k^2(M_3 + iM_4)\alpha\right] \end{aligned}\right\} \tag{39}$$

where $\alpha_h = \dot{h}/V$ is the angle of attack due to vertical translation. From equations (39) the section lift- and moment-curve slopes (complex derivatives) associated with vertical translation and pitching are, respectively,

$$\frac{dc_l}{d\alpha_h} = -i4k(L_1 + iL_2) \qquad \frac{dc_m}{d\alpha_h} = i2k(M_1 + iM_2) \tag{40a}$$

and

$$\frac{dc_l}{d\alpha} = 4k^2\left(L_3 + iL_4\right) \qquad \frac{dc_m}{d\alpha} = -2k^2\left(M_3 + iM_4\right) \tag{40b}$$

The coefficients c_l and c_m and their associated slopes reduce to well-known results in the steady case ($k = 0$). For example, substitution of the components given in equations (31) into equations (39) yields the result $c_l = 4\alpha/\beta$ (Ackeret's result) for a nonoscillating two-dimensional wing. Equations (39) and (40) have the additional feature that multiplying the components L_i and M_i ($i = 1$ and 2) associated with vertical translation by k and the components L_i and M_i ($i = 3$ and 4) associated with pitching by k^2 makes these quantities more uniform in magnitude and therefore more suitable for plotting.

Now consider the coefficients for total lift C_L and total moment C_m that may be obtained from equations (36) as

$$\left.\begin{aligned} C_L &= -\frac{\bar{P}}{2\rho b^2 V^2 A} = 4\left[-ik\left(\bar{L}_1 + i\bar{L}_2\right)\alpha_h + k^2\left(\bar{L}_3 + i\bar{L}_4\right)\alpha\right] \\ C_m &= \frac{\bar{M}_\alpha}{4\rho b^3 V^2 A} = -2\left[-ik\left(\bar{M}_1 + i\bar{M}_2\right)\alpha_h + k^2\left(\bar{M}_3 + i\bar{M}_4\right)\alpha\right] \end{aligned}\right\} \tag{41}$$

From equations (41) the total lift- and moment-curve slopes (complex derivatives) associated with vertical translation and pitching are, respectively,

$$\frac{dC_L}{d\alpha_h} = -i4k\left(\bar{L}_1 + i\bar{L}_2\right) \qquad \frac{dC_m}{d\alpha_h} = i2k\left(\bar{M}_1 + i\bar{M}_2\right) \tag{42a}$$

and

$$\frac{dC_L}{d\alpha} = 4k^2\left(\bar{L}_3 + i\bar{L}_4\right) \qquad \frac{dC_m}{d\alpha} = -2k^2\left(\bar{M}_3 + i\bar{M}_4\right) \tag{42b}$$

Equations (40) may be used to illustrate the extent to which the approximate expressions of the present paper for the section force and moment on a finite rectangular wing may be useful. A comparison, based

on these equations, is made in figure 4 of some exact and approximate calculations for a two-dimensional wing vertically translating and pitching about its midchord position. Results for a two-dimensional wing are chosen because in this case approximate and exact results can be compared and the extent of convergence determined. The two-dimensional case is a legitimate standard in the absence of exact results for the finite wing since consideration of equation (16) will show that this equation is at least as convergent when expanded to a certain power of $\bar{\omega}$ for a finite wing as when expanded to the same power of $\bar{\omega}$ for a two-dimensional wing. In figure 4 the components of the section moment-curve slopes defined in equations (40) are plotted against $\bar{\omega}$ for $M = 10/9$ and $x_o = 0.5$. The three dashed-line curves appearing in each of the four parts of figure 4 represent approximate results obtained by substituting the components given in equations (32) into the appropriate expressions of equations (40) and retaining terms involving $\bar{\omega}$ up to the third, fifth, and seventh powers. The solid-line curves represent exact results obtained by using the moment coefficients tabulated in reference 3. Curves of the components of the section lift-curve slope are not included because they show essentially the same convergence tendencies.

As may be noted in figure 4, the value of $\bar{\omega}$ at which a particular approximation departs from the exact theory is essentially the same regardless of the moment component considered. By extending the $\bar{\omega}^3$ results of reference 1 (represented by the curves in fig. 4 labeled "expansion to $\bar{\omega}^3$," except that in the present paper an $\bar{\omega}^3$ term has been added to the component $2kM_1$) to $\bar{\omega}^5$ and to $\bar{\omega}^7$, the value of $\bar{\omega}$ at which the approximation and the exact theory depart at $M = 10/9$ has been increased from 0.8 to 1.3 and 2.0, respectively. Further investigation will show that these values of $\bar{\omega}$ remain essentially the same regardless of the Mach number involved. The ranges of reduced frequency k $\left(\text{equal to } \frac{\bar{\omega}}{2}\frac{M^2 - 1}{M^2}\right)$ in which the various approximations adequately represent the exact theory may therefore be expressed as follows:

For expansion to $\bar{\omega}^3$,

$$0 \leqq k \leqq \frac{0.4(M^2 - 1)}{M^2}$$

for expansion to $\bar{\omega}^5$,

$$0 \leqq k \leqq \frac{0.65(M^2 - 1)}{M^2}$$

and for expansion to $\bar{\omega}^7$,

$$0 \leqq k \leqq \frac{1.0\left(M^2 - 1\right)}{M^2}$$

From these expressions it is readily seen that expanding to $\bar{\omega}^7$ rather than $\bar{\omega}^3$ more than doubles the allowable k range. For example, at $M = 10/9$ the limiting value of k is increased from 0.076, which is too small, to 0.19 which is sufficiently large to include most flutter cases that would likely be encountered at this Mach number.

In order to study the effect of aspect ratio on the forces and moments, consideration is given to the spanwise variation of section lift and moment coefficients. The curves in figures 5 and 6 serve as illustrations. In figure 5 the magnitudes of the slopes obtained by substituting equations (29) to (32) into equations (40) are plotted against the spanwise variable $1 - \zeta$ for the conditions $M = 1.3$, $A = 4$, $x_o = 0.413$, and $\bar{\omega} = 0.544$. The quantity ζ is the previously used variable y divided by $A/2$. The phase angles associated with the magnitudes of the slopes shown in figure 5 are plotted in figure 6; for example, the phase angle associated with the magnitude $\left|\frac{dc_l}{d\alpha}\right| = 4k^2\sqrt{L_3^2 + L_4^2}$ is $\theta_\alpha = \tan^{-1} L_4/L_3$. The portions of the curves in these figures in the range $0 \leqq 1 - \zeta \leqq 0.4$ $(1/\beta \leqq y \leqq A/2)$ also apply to a two-dimensional wing under the conditions listed. The effect of aspect ratio may be noted in the tip region $0.4 < 1 - \zeta \leqq 1.0$ $(0 \leqq y < 1/\beta)$.

The phase angles θ_h and $\theta_{\alpha m}$ in figure 6 are of particular interest. In keeping with the fact that a component of the force due to h in phase with the velocity $\dot{h}$ or a component of the moment due to α in phase with the angular velocity $\dot{\alpha}$ would be destabilizing, values of θ_h between 90° and 270° and values of $\theta_{\alpha m}$ between 0° and 180° would indicate possible dynamic instability in pure bending and pure torsion, respectively. The coefficient L_2, however, is always positive so that θ_h is between -90° and 90°; this agrees with the well-known fact that pure bending oscillations are always damped, at least in potential flow. The phase angle $\theta_{\alpha m}$, on the other hand, is less than 180° in the two-dimensional region and corresponds to undamped or unstable conditions; whereas in most of the region affected by the wing tip the phase angle $\theta_{\alpha m}$ is greater than 180°, which corresponds to damped or

stable conditions. The main feature of figure 6, therefore, is that aspect ratio has a stabilizing effect with regard to the motion α. This result seems to indicate that a flutter analysis which takes into account the spanwise variation of aerodynamic forces would yield a higher flutter-speed coefficient than one based on two-dimensional aerodynamic forces.

Upon substituting equations (37) and (38) into equations (42), the overall effect of aspect ratio on the total lift- and moment-curve slopes can be calculated for particular values of the parameters M, $\bar{\omega}$, x_o, and A. Although the effect of aspect ratio A may change considerably with small changes in one or more of the other parameters, some insight into the overall effect may be gained from calculations in which, together with A, one of the parameters $\bar{\omega}$, x_o, or M is varied while the other two remain fixed. Figures 7 and 8 show the effect on $dC_L/d\alpha$ and $dC_m/d\alpha$ of varying A and $\bar{\omega}$ while keeping M and x_o fixed, and figure 9 shows the effect on $dC_m/d\alpha$ of varying A and x_o while keeping M and $\bar{\omega}$ fixed. The effect on the total lift- and moment-curve slopes of varying A and M can be extracted from figures 4 and 5 of reference 1.

In figure 7 the magnitudes and in figure 8 the associated phase angles of the slopes $dC_L/d\alpha$ and $dC_m/d\alpha$ are plotted against $\bar{\omega}$ for $M = 1.3$, $x_o = 0.5$, and several values of A. In figure 9 the limiting value as $\bar{\omega} \longrightarrow 0$ of the slope $dC_m/d\alpha$ is plotted against x_o for $M = 1.3$ and three values of A. The curves in figures 7, 8, and 9 labeled $A = 1/\beta$ apply to the least value of A permitted by the foregoing analysis in that they represent calculations for the combination of aspect ratio and Mach number that causes the Mach line from one wing tip to intersect the opposite tip at the trailing edge.

As illustrated in figure 7(a), a decrease in aspect ratio for a given value of $\bar{\omega}$ produces a decrease in the magnitude of the total lift-curve slope. This trend is in general true for the range of $\bar{\omega}$ considered and is not affected by a change in x_o or M (see fig. 4 of ref. 1). In the case of the magnitude of the total moment-curve slope, however, the trend with aspect ratio is greatly dependent on x_o. As may be seen from figures 7(b) and 9 (see also fig. 5 of ref. 1), the magnitude may increase, decrease, or perhaps not vary at all (as is the case in fig. 9 at $x_o = 0.67$) with a decrease in aspect ratio, depending on the value of x_o under consideration. This seemingly anomalous behavior of the total moment-curve slope is associated with the change in center of pressure, for prescribed motions of the wing, with change in aspect ratio. Also note in figures 7 and 9 that the departure from the two-dimensional ($A = \infty$) results is rather large for aspect ratios less than about 4.

From figure 9 for $A = \infty$ the following phase angles are obtained: $\theta_{AM} = 180^\circ$ for $x_o < 0.5$ and $\theta_{AM} = 0^\circ$ for $x_o > 0.5$. The phase angle of 90° shown in figure 8(b) for $A = \infty$, $\bar{\omega} = 0$, and $x_o = 0.5$, although associated with a slope of zero magnitude and not really significant, is therefore a transitional value. Note in figure 8(b) that θ_{AM} is less than 0° for A less than 6; this result also indicates that aspect ratio is stabilizing.

APPLICATION OF FORCES AND MOMENTS TO FLUTTER

Method of Flutter Analysis

For the purpose of applying the foregoing results, a flutter analysis of the Rayleigh type for uniform cantilever wings is now considered. Such an analysis involves the selection of a set of modal functions to approximate the flutter mode, the formation of the flutter determinant, and the solution of this determinant for the flutter condition. (Although the use of the force and moment coefficients derived herein for the undistorted rectangular wing results, in certain cases, in a big improvement in accuracy over the use of two-dimensional flow coefficients, perhaps a more accurate but much more cumbersome procedure would be to use coefficients derived for a distorted wing.)

The flutter mode of the uniform cantilever wing is assumed to be adequately represented by proper combination of the uncoupled first bending and first torsion mode shapes of the wing. The flutter determinant based on these two modes has the form

$$\begin{vmatrix} A_{hh} & A_{h\alpha} \\ A_{\alpha h} & A_{\alpha\alpha} \end{vmatrix} = 0 \tag{43}$$

where the determinant elements are given by (see fig. 10 for coordinate ζ)

$$A_{hh} = \left[1 - \left(\frac{\omega_h}{\omega}\right)^2\right] \int_0^1 Z_h^2 \, d\zeta - \frac{4}{\pi} \kappa \int_0^1 \left(L_1 + iL_2\right) Z_h^2 \, d\zeta \tag{44a}$$

$$A_{h\alpha} = x_\alpha \int_0^1 Z_h Z_\alpha \, d\zeta - \frac{4}{\pi} \kappa \int_0^1 \left(L_3 + iL_4\right) Z_h Z_\alpha \, d\zeta \tag{44b}$$

$$A_{\alpha h} = x_\alpha \int_0^1 Z_\alpha Z_h \, d\zeta - \frac{4}{\pi} \kappa \int_0^1 \left(M_1 + iM_2\right) Z_\alpha Z_h \, d\zeta \tag{44c}$$

$$A_{\alpha\alpha} = r_\alpha^2 \left[1 - \left(\frac{\omega_\alpha}{\omega}\right)^2\right] \int_0^1 Z_\alpha{}^2 d\zeta - \frac{4}{\pi} \kappa \int_0^1 \left(M_3 + iM_4\right) Z_\alpha{}^2 d\zeta \tag{44d}$$

and where ω is the flutter frequency. In the event that two-dimensional air forces and moments are used, the force and moment coefficients appear as constants in the integrals and can be factored from under the integral signs, and the determinant elements become

$$\left.\begin{aligned}
A_{hh} &= \left\{\left[1 - \left(\frac{\omega_h}{\omega}\right)^2\right] - \frac{4}{\pi} \kappa \left(L_1 + iL_2\right)\right\} \int_0^1 Z_h{}^2 d\zeta \\
A_{h\alpha} &= \left[x_\alpha - \frac{4}{\pi} \kappa \left(L_3 + iL_4\right)\right] \int_0^1 Z_h Z_\alpha \, d\zeta \\
A_{\alpha h} &= \left[x_\alpha - \frac{4}{\pi} \kappa \left(M_1 + iM_2\right)\right] \int_0^1 Z_\alpha Z_h \, d\zeta \\
A_{\alpha\alpha} &= \left\{r_\alpha^2 \left[1 - \left(\frac{\omega_\alpha}{\omega}\right)^2\right] - \frac{4}{\pi} \kappa \left(M_3 + iM_4\right)\right\} \int_0^1 Z_\alpha{}^2 d\zeta
\end{aligned}\right\} \tag{45}$$

(It may be noted that eqs. (44) and (45) are not restricted to any particular Mach number range if L_i and M_i ($i = 1, 2, 3,$ and 4) defined in accordance with eq. (28) are taken to apply at either subsonic or supersonic speed.) The uncoupled first bending mode shape Z_h and the first torsion mode shape Z_α needed for the evaluation of the aerodynamic integrals of equations (44) are plotted against $1 - \zeta$ in figure 11. The mode-shape integrals of equations (44) and (45) are given by

$$\int_0^1 Z_h{}^2 d\zeta = 0.25$$

$$\int_0^1 Z_h Z_\alpha \, d\zeta = 0.337$$

$$\int_0^1 Z_\alpha^2 d\zeta = 0.50$$

The flutter condition is determined from the nontrivial solution of equation (43). This solution may be obtained by various means (see ch. XIII of ref. 7). In the present paper equation (43) was solved for the unknown ω_h/ω_α. For a particular wing and Mach number, for which values of M, κ, x_o, x_α, r_α^2, and ω_h/ω_α are specified, the reduced frequency k was varied until the ratio ω_h/ω_α determined from equation (31) matched that of the wing. In this manner the values of k and ω_α/ω at flutter and consequently the flutter-speed coefficient $V/b\omega_\alpha$ were determined for the wing at the selected value of M.

Flutter Calculations

The foregoing method of analysis was used to obtain flutter characteristics in the Mach number range $10/9 \leqq M \leqq 10/6$ for a rectangular wing with the following properties: $A = 4.53$, $1/\kappa = 95.3$, $x_o = 0.341$, $x_\alpha = 0.350$, $r_\alpha^2 = 0.39$, and $\omega_h/\omega_\alpha = 0.583$. Calculations were made on the basis of the components of the section force and moment coefficients given in equations (29) to (32). A numerical method for evaluating the aerodynamic integrals resulting from the use of these components (for example, $\int_0^1 (L_1 + iL_2) Z_h^2 d\zeta$ in eq. (44a)) is outlined in appendix B. For comparison, calculations were also made by using force and moment coefficients for a two-dimensional wing (strip theory). In this latter case the determinant elements are of the form given in equations (45) wherein the components L_i and M_i are obtained from either reference 3 or equations (31) and (32) of the present paper. In figure 12 the two curves resulting from these calculations are plotted in the form of flutter-speed coefficient $V/b\omega_\alpha$ against Mach number M. As may be noted in the figure, the curves are well-separated at $M = 10/9$ but tend to converge as the Mach number is increased. At $M = 10/9$ the flutter speed obtained by using coefficients for a two-dimensional wing is about 62 percent of that obtained by using coefficients for a rectangular wing, whereas at $M = 10/6$ it is about 95 percent.

CONCLUDING REMARKS

The linearized theory for compressible unsteady flow has been used to derive expressions to the seventh power of the frequency of oscillation for the velocity potential and section and total forces and moments for a thin rectangular wing harmonically oscillating in pitch and vertical translation and moving at supersonic speed. These expressions are extensions, although obtained by a different method, of similar expressions derived to the third power of the frequency of oscillation in NACA Report 1028. As a result of this extension the largest value of reduced frequency for which the theory is sufficiently exact has been increased from $k = \frac{0.4(M^2 - 1)}{M^2}$ to $k = \frac{M^2 - 1}{M^2}$, where M is the Mach number. For example, at $M = 10/9$ expansion to the third power of the frequency is accurate up to about $k = 0.08$, whereas expansion to the seventh power is accurate up to $k = 0.2$. The first of these values for k is too small but the second is probably large enough to include most rectangular-wing flutter cases likely to occur at $M = 10/9$.

Flutter calculations were made in the Mach number range from 10/9 to 10/6 for a rectangular wing of aspect ratio 4.53 by using the section force and moment coefficients for a rectangular wing derived in the present paper and the force and moment coefficients for a two-dimensional wing given in NACA Report 846. Comparison of the two curves of flutter speed indicated, as may be expected, that the use of finite-wing coefficients is very influential at Mach numbers near unity but becomes less so as the Mach number is increased. At $M = 10/9$ for the particular wing analyzed, the flutter speed obtained by using the section coefficients for a two-dimensional wing is about 62 percent of that obtained by using coefficients for a rectangular wing; whereas at $M = 10/6$ it is about 95 percent. Since flutter speeds calculated on the basis of two-dimensional-wing coefficients are generally very conservative in the low supersonic speed range, it would seem that flutter speeds obtained by using the section coefficients for rectangular wings of the present paper may compare more favorably with experiment.

Langley Aeronautical Laboratory,
National Advisory Committee for Aeronautics,
Langley Field, Va., January 14, 1954.

APPENDIX A

SOME INTEGRATED VALUES OF F_n AND $\bar{\bar{F}}_n$

From equation (19) the values of the functions F_n needed in equation (22) are as follows:

$$F_1 = \sqrt{\beta y(x - \beta y)} + x \sin^{-1}\sqrt{\beta y/x}$$

$$F_2 = \frac{x + 2\beta y}{6}\sqrt{\beta y(x - \beta y)} + \frac{x^2}{2}\sin^{-1}\sqrt{\beta y/x}$$

$$F_3 = \frac{3x^2 + 4\beta yx + 8\beta^2y^2}{45}\sqrt{\beta y(x - \beta y)} + \frac{x^3}{3}\sin^{-1}\sqrt{\beta y/x}$$

$$F_4 = \frac{5x^3 + 6\beta yx^2 + 8\beta^2y^2x + 16\beta^3y^3}{140}\sqrt{\beta y(x - \beta y)} + \frac{x^4}{4}\sin^{-1}\sqrt{\beta y/x}$$

$$F_5 = \frac{35x^4 + 40\beta yx^3 + 48\beta^2y^2x^2 + 64\beta^3y^3x + 128\beta^4y^4}{1575}\sqrt{\beta y(x - \beta y)} + \frac{x^5}{5}\sin^{-1}\sqrt{\beta y/x}$$

$$F_6 = \frac{63x^5 + 70\beta yx^4 + 80\beta^2y^2x^3 + 96\beta^3y^3x^2 + 128\beta^4y^4x + 256\beta^5y^5}{4158}\sqrt{\beta y(x - \beta y)} + \frac{x^6}{6}\sin^{-1}\sqrt{\beta y/x}$$

$$F_7 = \frac{231x^6 + 252\beta yx^5 + 280\beta^2y^2x^4 + 320\beta^3y^3x^3 + 384\beta^4y^4x^2 + 512\beta^5y^5x + 1024\beta^6y^6}{21021}\sqrt{\beta y(x - \beta y)} + \frac{x^7}{7}\sin^{-1}\sqrt{\beta y/x}$$

$$F_8 = \frac{429x^7 + 462x^6\beta y + 504x^5\beta^2y^2 + 560x^4\beta^3y^3 + 640x^3\beta^4y^4 + 768x^2\beta^5y^5 + 1024x\beta^6y^6 + 2048\beta^7y^7}{51480}\sqrt{\beta y(x - \beta y)} + \frac{x^8}{8}\sin^{-1}\sqrt{\beta y/x}$$

$$F_9 = \frac{6435x^8 + 6864x^7\beta y + 7392x^6\beta^2y^2 + 8064x^5\beta^3y^3 + 8960x^4\beta^4y^4 + 10240x^3\beta^5y^5 + 12288x^2\beta^6y^6 + 16384x\beta^7y^7 + 32768\beta^8y^8}{98455}\sqrt{\beta y(x - \beta y)} + \frac{x^9}{9}\sin^{-1}\sqrt{\beta y/x}$$

The functions F_1 to F_5 were given previously in reference 1 but are repeated here for the sake of completeness.

The values of $\bar{\bar{F}}_n$ needed in equations (29) and (30) are obtained by substituting the value of x at the trailing edge ($x = 1$) into the preceding values of F_n. That is,

$$\bar{\bar{F}}_n = F_n(1,y)$$

APPENDIX B

NUMERICAL METHOD OF EVALUATING AERODYNAMIC INTEGRALS IN FLUTTER DETERMINANT

A numerical method of integration for evaluating the aerodynamic integrals of equations (44) is now outlined. The outline is based on the two cases discussed after equation (28) and depicted in figure 3.

Case 1 (see fig. 3(a)): The spanwise stations at which values for the components of the section force and moment coefficients given in equations (29) to (32) are to be found are shown in figure 10. Since equations (29) and (30) reduce, respectively, to equations (31) and (32) for $\zeta \geq 2/A\beta$, the values of $\bar{\bar{F}}_n$ needed to obtain the components of the section force and moment coefficients at the various stations are as follows:

Station	ζ	y	$\sqrt{\beta y(1 - \beta y)}$	$\sin^{-1}\sqrt{\beta y}$	$\bar{\bar{F}}_1$	$\bar{\bar{F}}_2$	$\bar{\bar{F}}_3$	$\bar{\bar{F}}_4$	$\bar{\bar{F}}_5$	$\bar{\bar{F}}_6$	$\bar{\bar{F}}_7$	$\bar{\bar{F}}_8$	$\bar{\bar{F}}_9$
0	0	0	0	0	0	0	0	0	0	0	0	0	0
1	λ_β	$1/4\beta$	$\sqrt{3}/4$	$\pi/6$	.95661	.37005	.21783	.15332	.11833	.09640	.08137	.07040	.06204
2	$2\lambda_\beta$	$1/2\beta$	1/2	$\pi/4$	1.28540	.55937	.33958	.23921	.18343	.14846	.12464	.10742	.09440
3	$3\lambda_\beta$	$3/4\beta$	$\sqrt{3}/4$	$\pi/3$	1.48021	.70402	.45010	.32598	.25329	.20601	.17304	.14562	.13046
4, 5, 6	$\geq 4\lambda_\beta$	$\geq 1/\beta$	0	$\pi/2$	1.57080	.78540	.52360	.39270	.31416	.26180	.22440	.19635	.17453

Note that these values of $\bar{\bar{F}}_n$ do not vary with A and β so long as $A\beta > 2$. From the expressions for L_1 and L_2 in equation (29), the preceding table of values of $\bar{\bar{F}}_n$, the curve for Z_h in figure 11, and the flutter parameters

$$k = 0.10 \qquad A = 4$$

$$\beta = 0.8307 \qquad \lambda_\beta = \frac{1}{2A\beta} = 0.1505$$

$$x_o = 0.431 \qquad \lambda = 0.5 - \frac{1}{A\beta} = 0.1990$$

the following sample integration table based on Simpson's parabolic integrating rule may be devised:

Station, n	ζ	Z_h^2	$L_1 + iL_2$	$I_n = (L_1 + iL_2)Z_h^2$
0	0	1.0000	0	0
1	.1505	.6273	.4549 + 7.1684i	.2854 + 4.4965i
2	.3010	.3469	.9335 + 9.5932i	.3238 + 3.3281i
3	.4515	.1584	1.3839 + 10.9939i	.2192 + 1.7415i
4	.6020	.0520	1.6646 + 11.6236i	.0865 + .6042i
5	.8010	.0041	1.6646 + 11.6236i	.0068 + .0476i
6	1.0000	0	1.6646 + 11.6236i	0

$$\int_0^1 (L_1 + iL_2)Z_h^2 d\zeta = \frac{\lambda\beta}{3}(I_0 + 4I_1 + 2I_2 + 4I_3 + I_4) + \frac{\lambda}{3}(I_4 + 4I_5 + I_6)$$

$$= 0.1456 + 1.6685i$$

where I_n denotes the value of the integrand at station n. In a similar manner the remaining aerodynamic integrals of equations (44) can be evaluated.

Case 2 (see fig. 3(b)): In this case, as illustrated by equation (33), the components of the force and moment coefficients for the wing sections passing through region T_3 contain the functions $\bar{\bar{F}}_n(A - y)$ in addition to the functions $\bar{\bar{F}}_n(y)$. As a result, there is no arrangement of spanwise stations which will yield values of $\bar{\bar{F}}_n$ that do not vary with A and β. For this reason, it seems advisable simply to choose stations at even increments along the span for the numerical integration.

REFERENCES

1. Watkins, Charles E.: Effect of Aspect Ratio on the Air Forces and Moments of Harmonically Oscillating Thin Rectangular Wings in Supersonic Potential Flow. NACA Rep. 1028, 1951.

2. Stewartson, K.: On Linearized Potential Theory of Unsteady Supersonic Motion. Quarterly Jour. Mech. and Appl. Math., vol. III, pt. 2, June 1950, pp. 182-199.

3. Garrick, I. E., and Rubinow, S. I.: Flutter and Oscillating Air-Force Calculations for an Airfoil in a Two-Dimensional Supersonic Flow. NACA Rep. 846, 1946. (Supersedes NACA TN 1158.)

4. Lamb, Horace: Hydrodynamics. Reprint of sixth ed. (first American ed.), Dover Publications, 1945, pp. 538-541.

5. Bateman, H.: Partial Differential Equations of Mathematical Physics. American ed., Dover Publications, 1944, p. 478.

6. Churchill, Ruel V.: Modern Operational Mathematics in Engineering. McGraw-Hill Book Co., Inc., 1944.

7. Scanlan, Robert H., and Rosenbaum, Robert: Introduction to the Study of Aircraft Vibration and Flutter. Ch. XIII, The Macmillan Co., 1951, pp. 265-297.

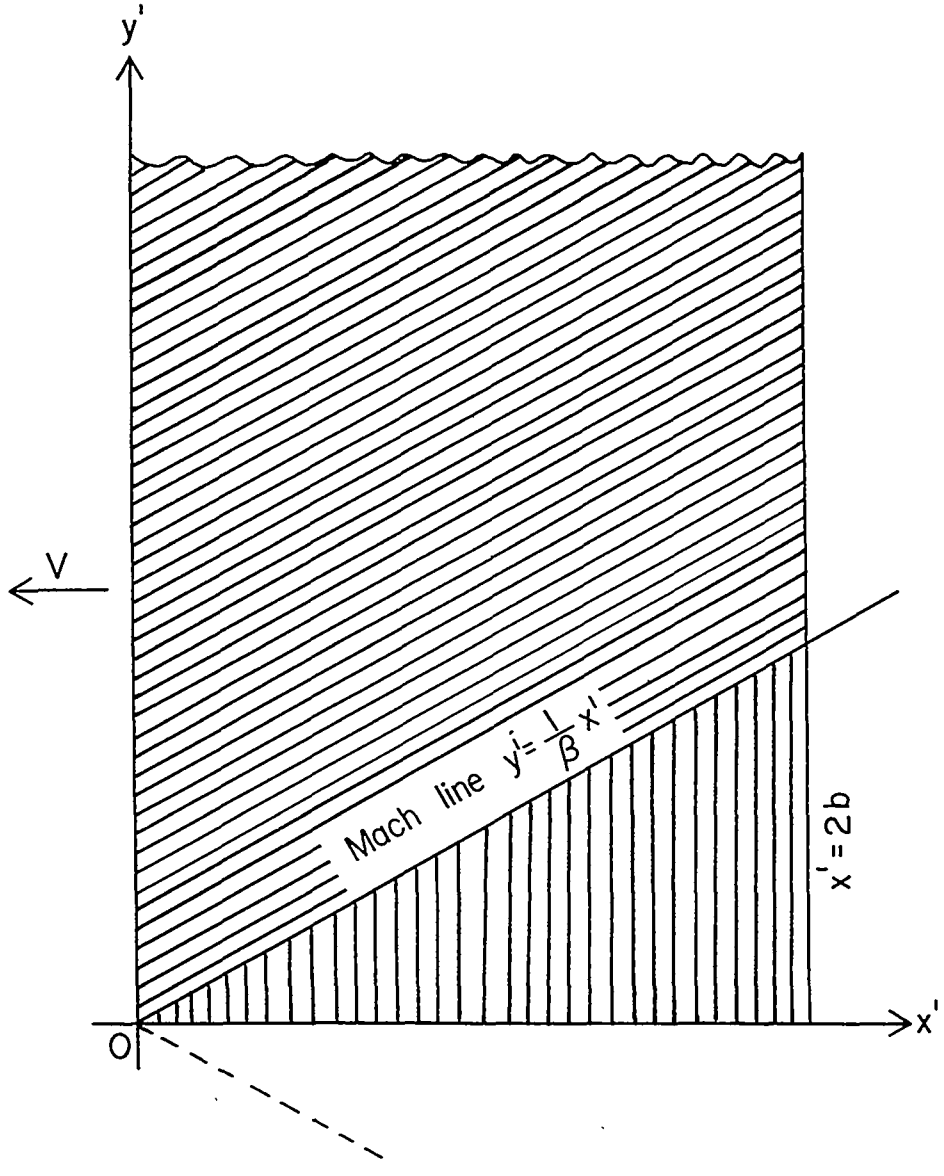

Figure 1.- Sketch illustrating chosen coordinate system for semi-infinite wing.

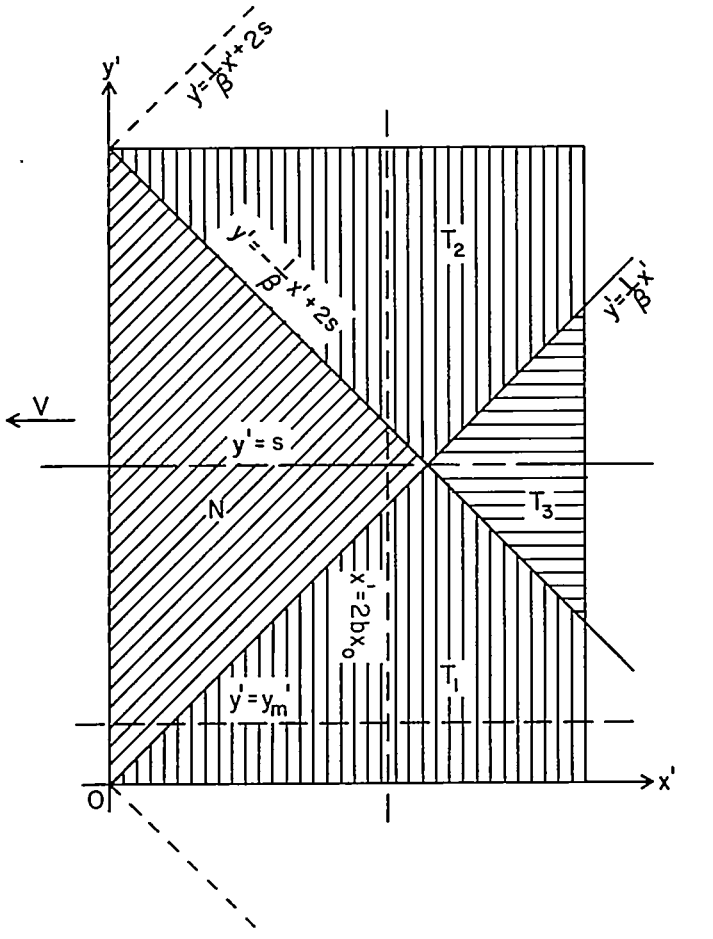

(a) Plan form (x'y'-plane).

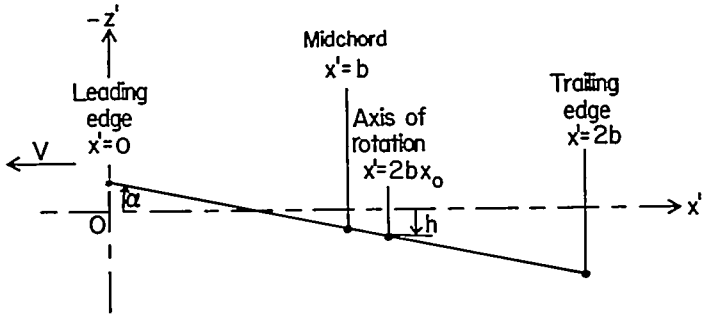

(b) Section $y'=y_m'$ (x'z'-plane).

Figure 2.- Sketch illustrating coordinate system for finite rectangular wing with two degrees of freedom α and h.

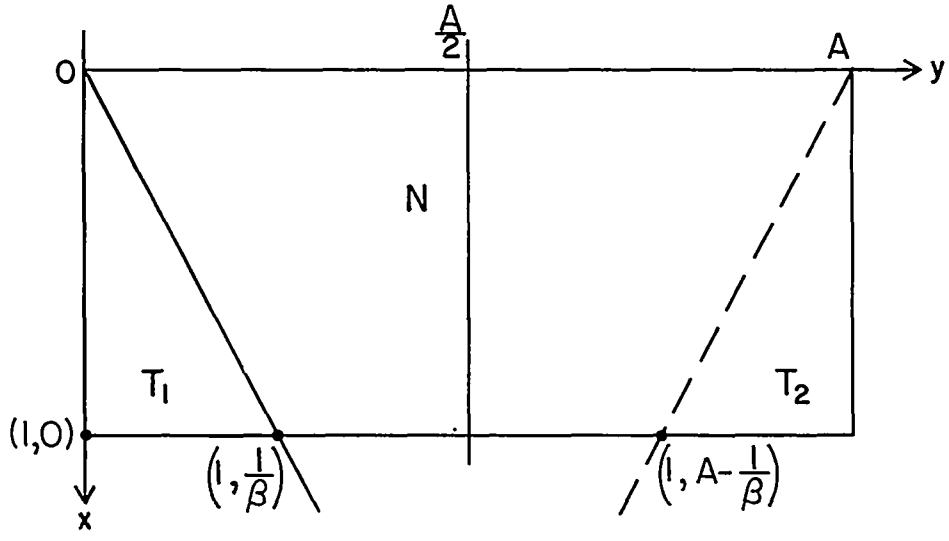

(a) Case 1.- Mach lines from tips do not intersect on wing ($A\beta > 2$).

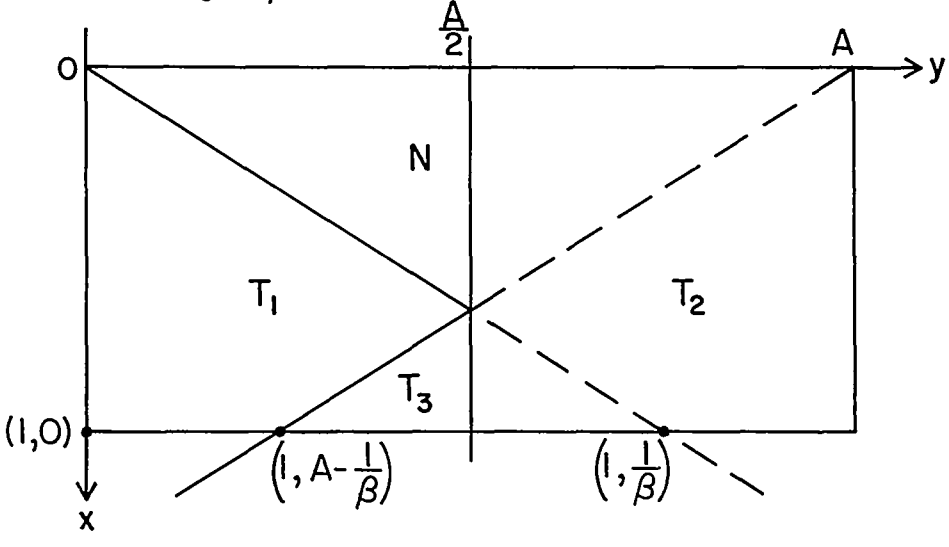

(b) Case 2.- Mach lines from tips intersect on wing but not ahead of midchord ($1 \leq A\beta \leq 2$).

Figure 3.- Sketch based on nondimensional coordinates x and y illustrating different Mach line locations accounted for in analysis.

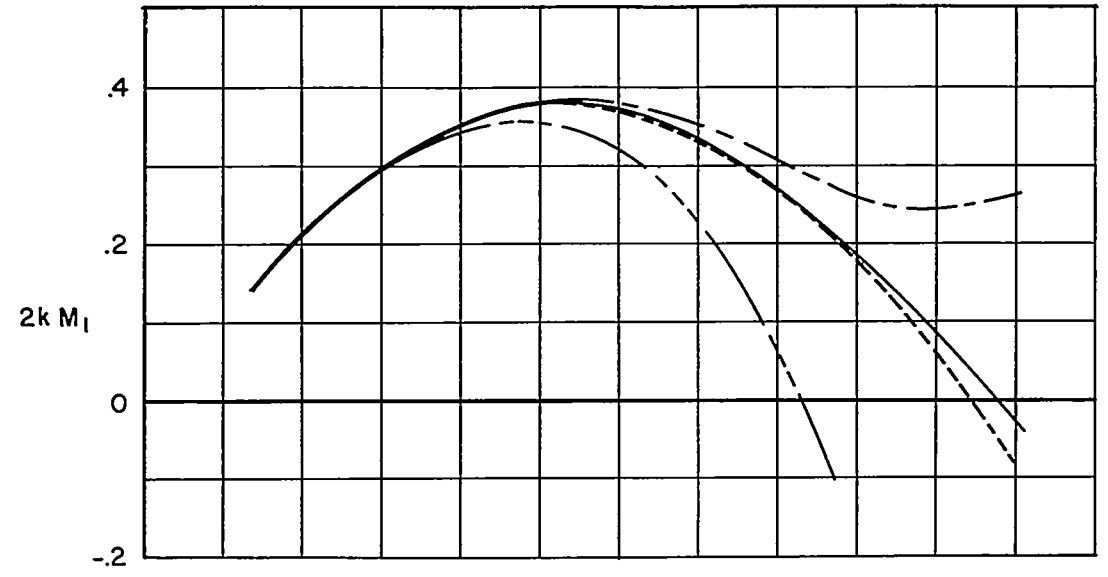

(a) Real part of moment-curve slope associated with vertical translation of wing.

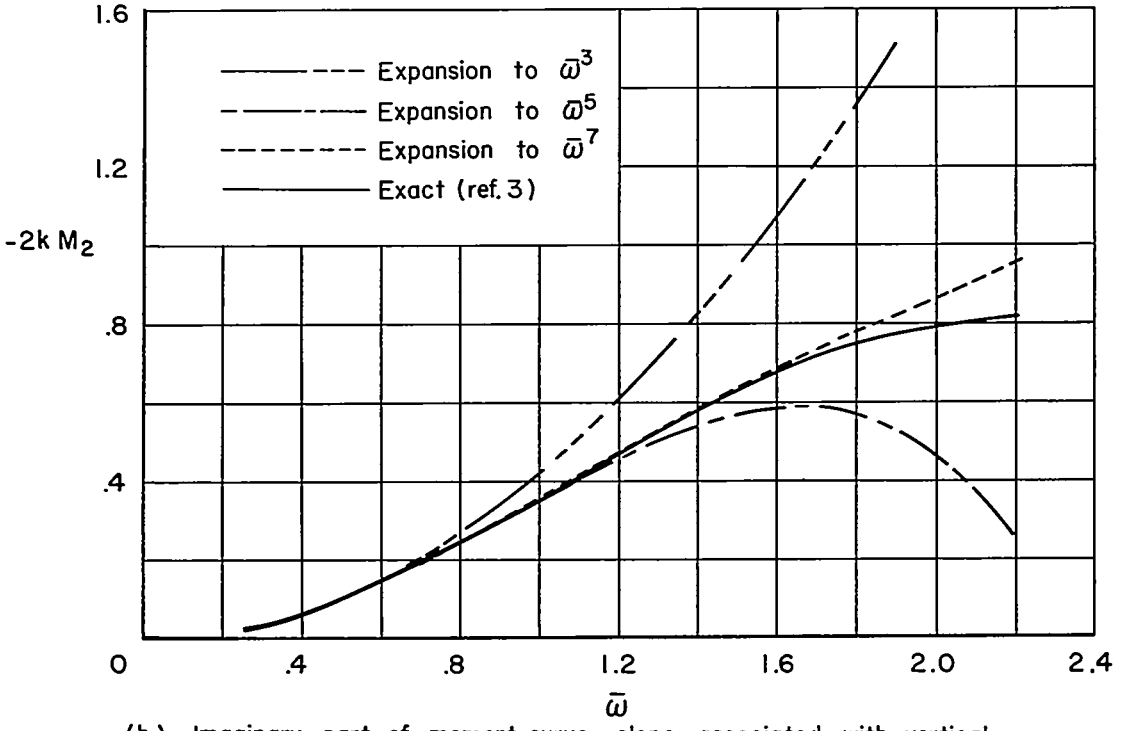

(b) Imaginary part of moment-curve slope associated with vertical translation of wing.

Figure 4.- Comparison of two-dimensional moment-curve slopes based on exact and approximate theory as a function of frequency parameter $\bar{\omega}$ for $M = 10/9$ and $x_o = 0.5$.

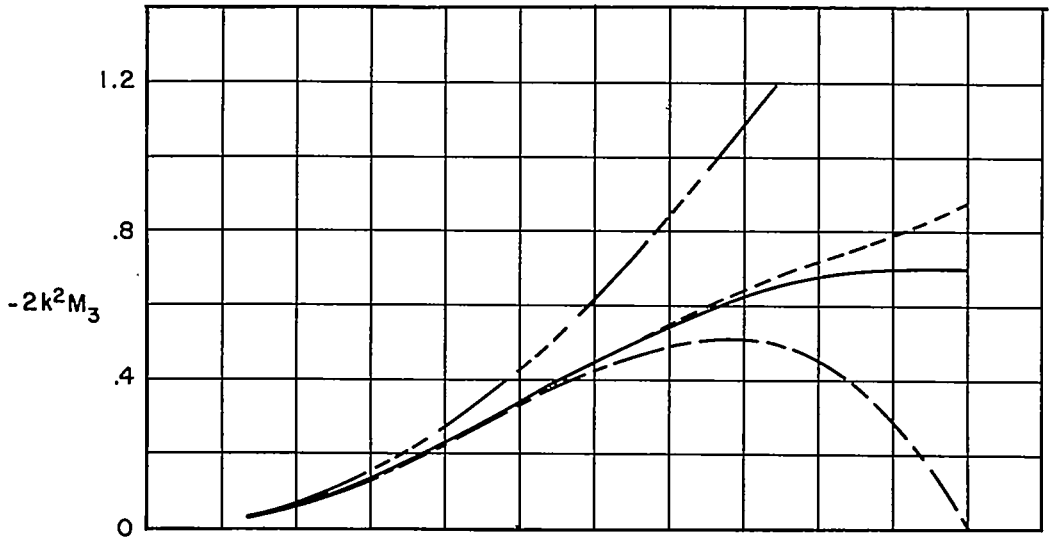

(c) Real part of moment-curve slope associated with pitching of wing.

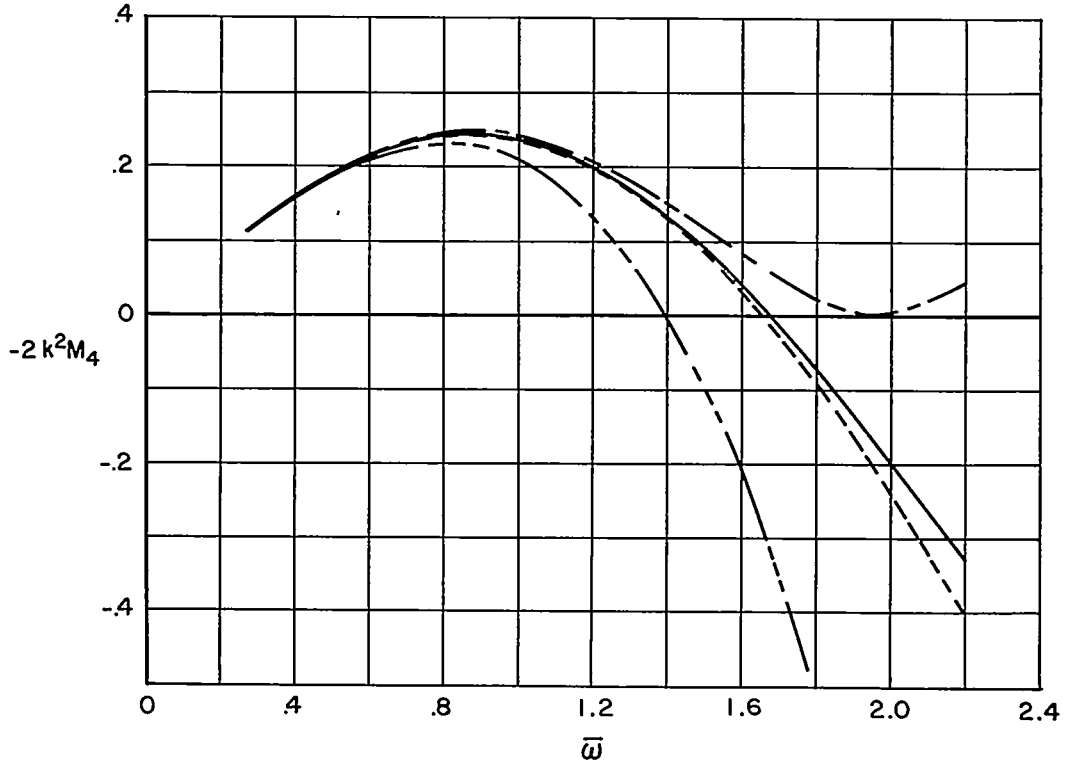

(d) Imaginary part of moment-curve slope associated with pitching of wing.

Figure 4.- Concluded.

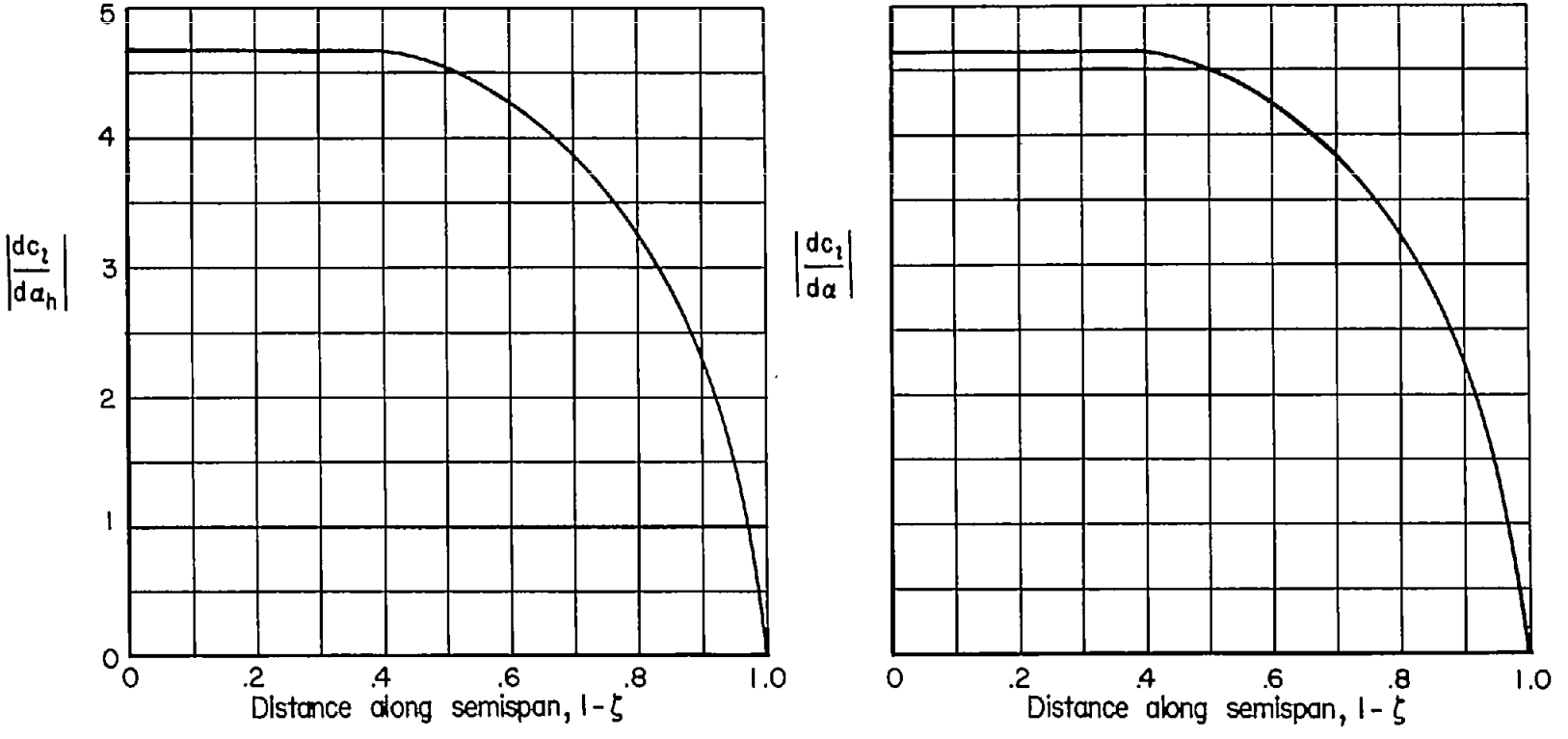

(a) Lift-curve slope associated with vertical translation of wing $\left|\frac{dc_l}{d\alpha_h}\right| = 4k\sqrt{L_1^2 + L_2^2}$.

(b) Lift-curve slope associated with pitching of wing $\left|\frac{dc_l}{d\alpha}\right| = 4k^2\sqrt{L_3^2 + L_4^2}$.

Figure 5.- Magnitudes of section lift-curve slope and section moment-curve slope for rectangular wing of aspect ratio 4 plotted against spanwise position in tenths of semispan measured from wing center for $M = 1.3$, $x_o = 0.413$, and $\mathfrak{B} = 0.544$.

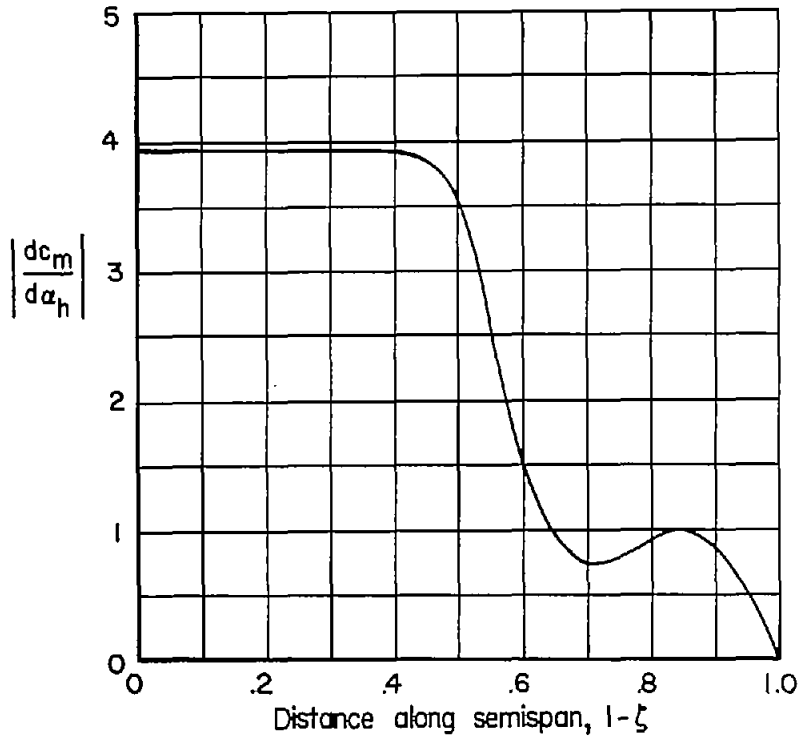

(c) Moment-curve slope associated with vertical translation of wing $\left|\frac{dc_m}{d\alpha_h}\right| = 2k\sqrt{M_1^2 + M_2^2}$

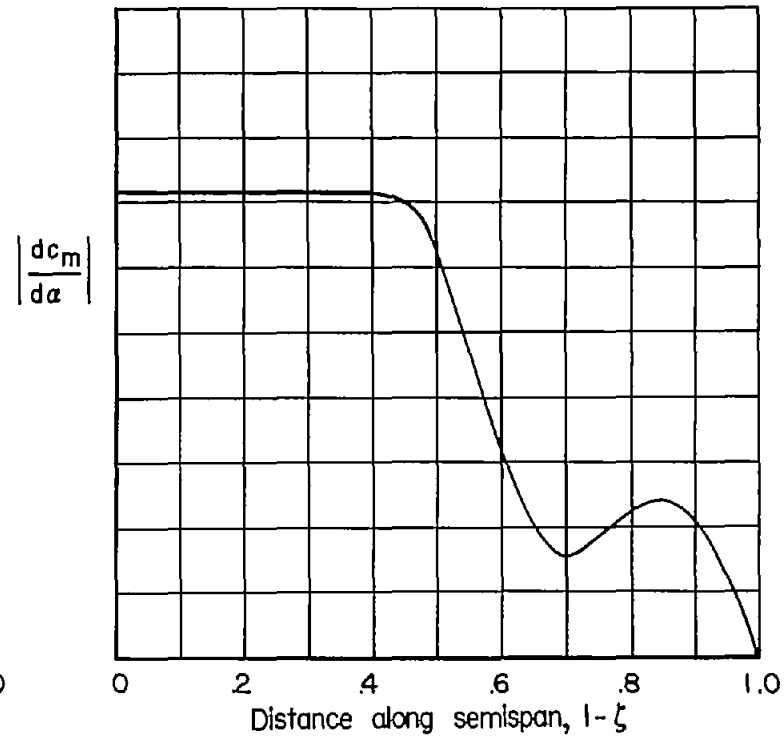

(d) Moment-curve slope associated with pitching of wing $\left|\frac{dc_m}{d\alpha}\right| = 2k^2\sqrt{M_3^2 + M_4^2}$.

Figure 5.- Concluded.

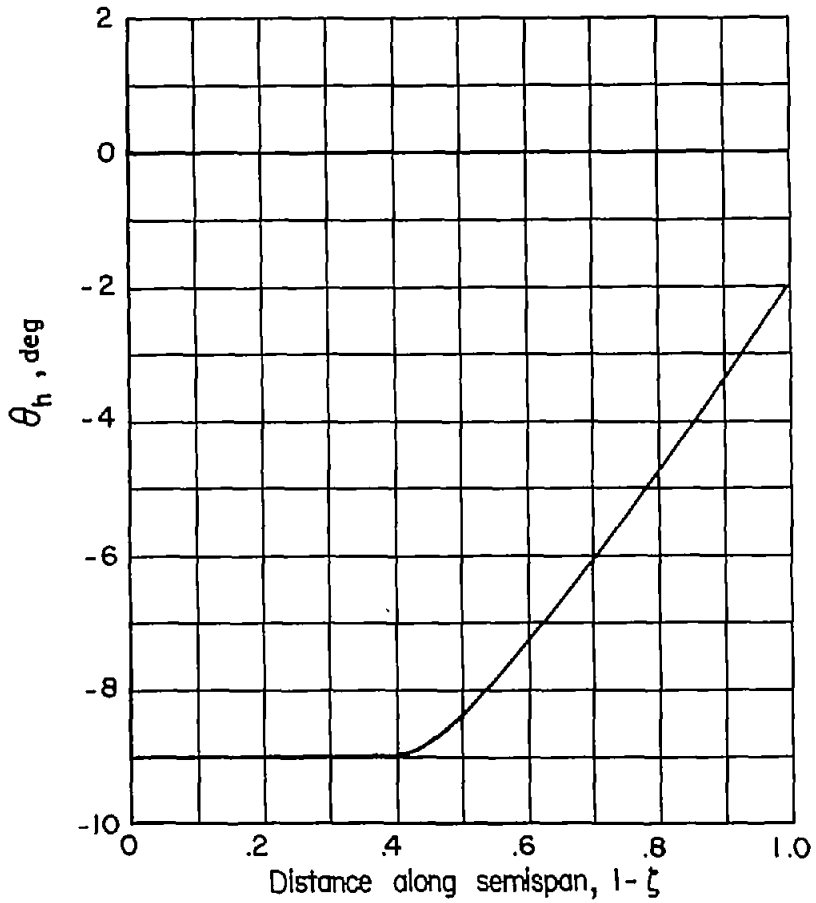

(a) Phase angle between lift vector due to vertical translation and vertical-velocity vector $\dot{h}$.

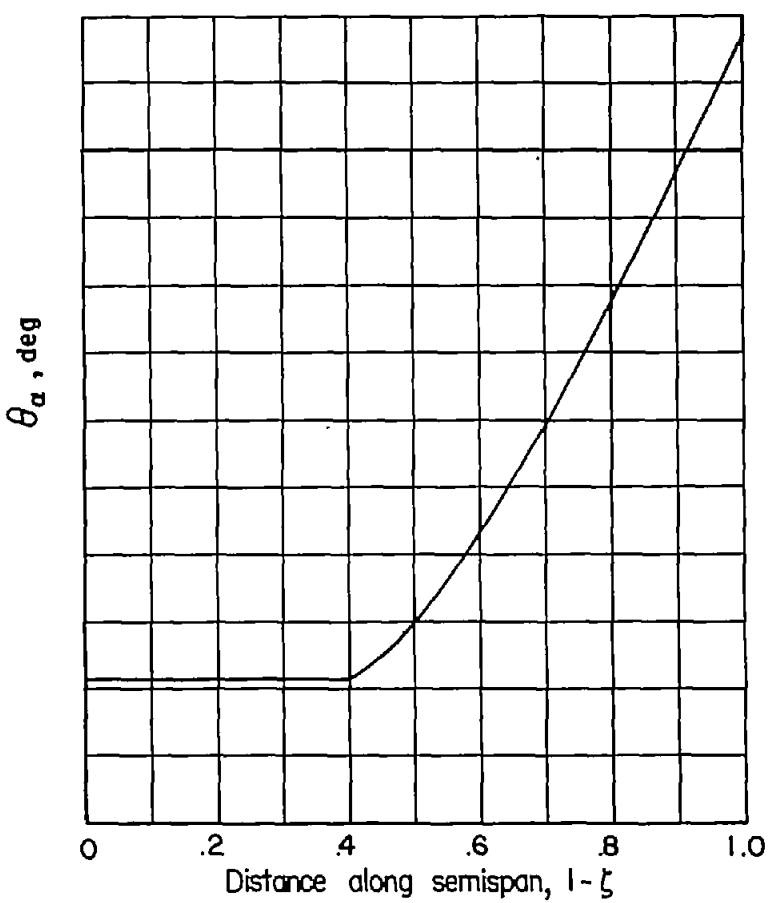

(b) Phase angle between lift vector due to pitching and angular-displacement vector α.

Figure 6.- Phase angles for rectangular wing of aspect ratio 4 plotted against spanwise position in tenths of semispan measured from wing center for $M = 1.3$, $x_o = 0.413$, and $\bar{\omega} = 0.544$.

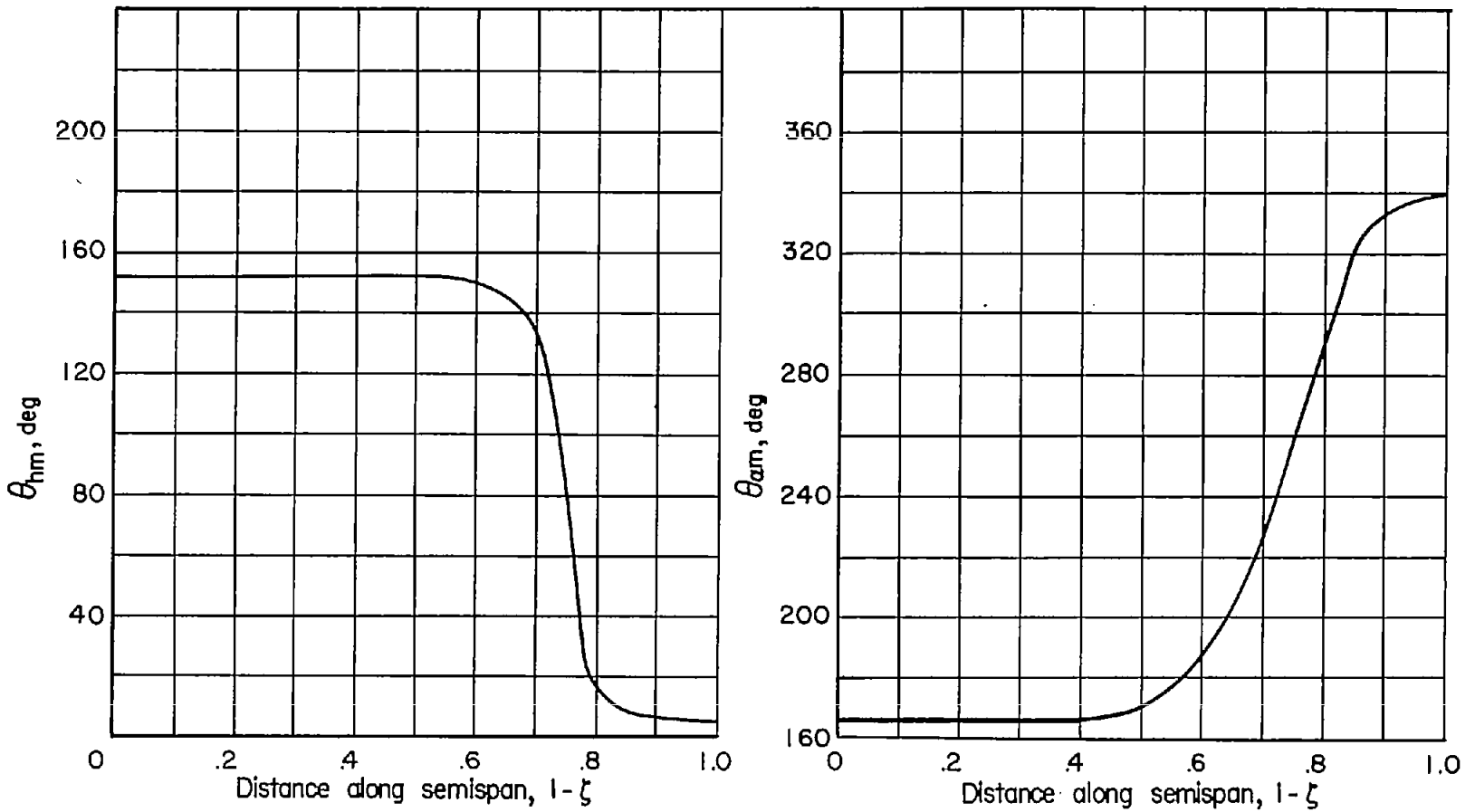

(c) Phase angle between moment vector due to vertical translation and vertical-velocity vector $\dot{h}$.

(d) Phase angle between moment vector due to pitching and angular-displacement vector α.

Figure 6.- Concluded.

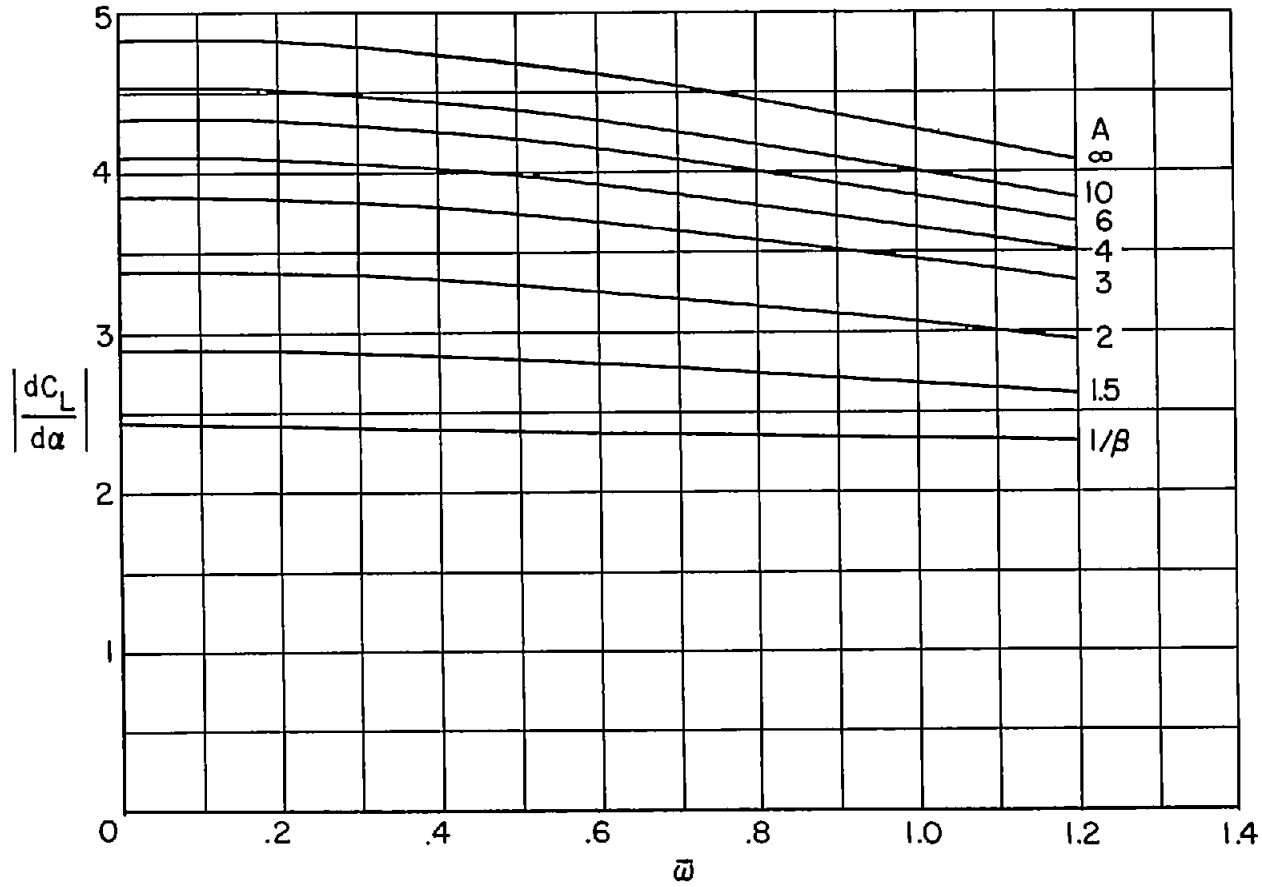

(a) Lift-curve slope $\left|\frac{dC_L}{d\alpha}\right| = 4k^2\sqrt{L_3^2 + L_4^2}$.

Figure 7.- Magnitudes of total lift-curve slope and total moment-curve slope associated with pitching as functions of $\bar{\omega}$ for $M = 1.3$, $x_o = 0.5$, and various values of A.

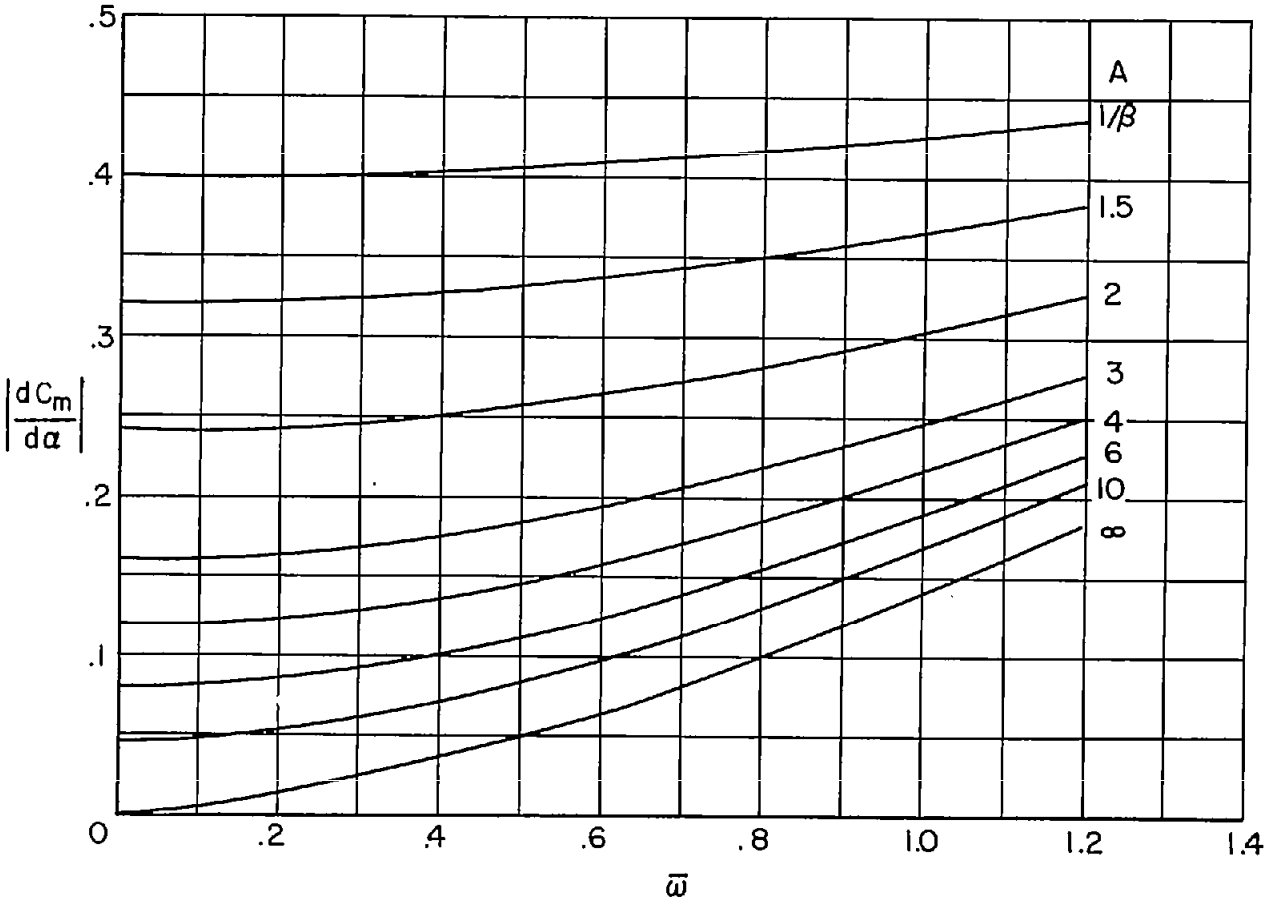

(b) Moment-curve slope $\left|\frac{dC_m}{d\alpha}\right| = 2k^2\sqrt{\bar{M}_3^2 + \bar{M}_4^2}$.

Figure 7.- Concluded.

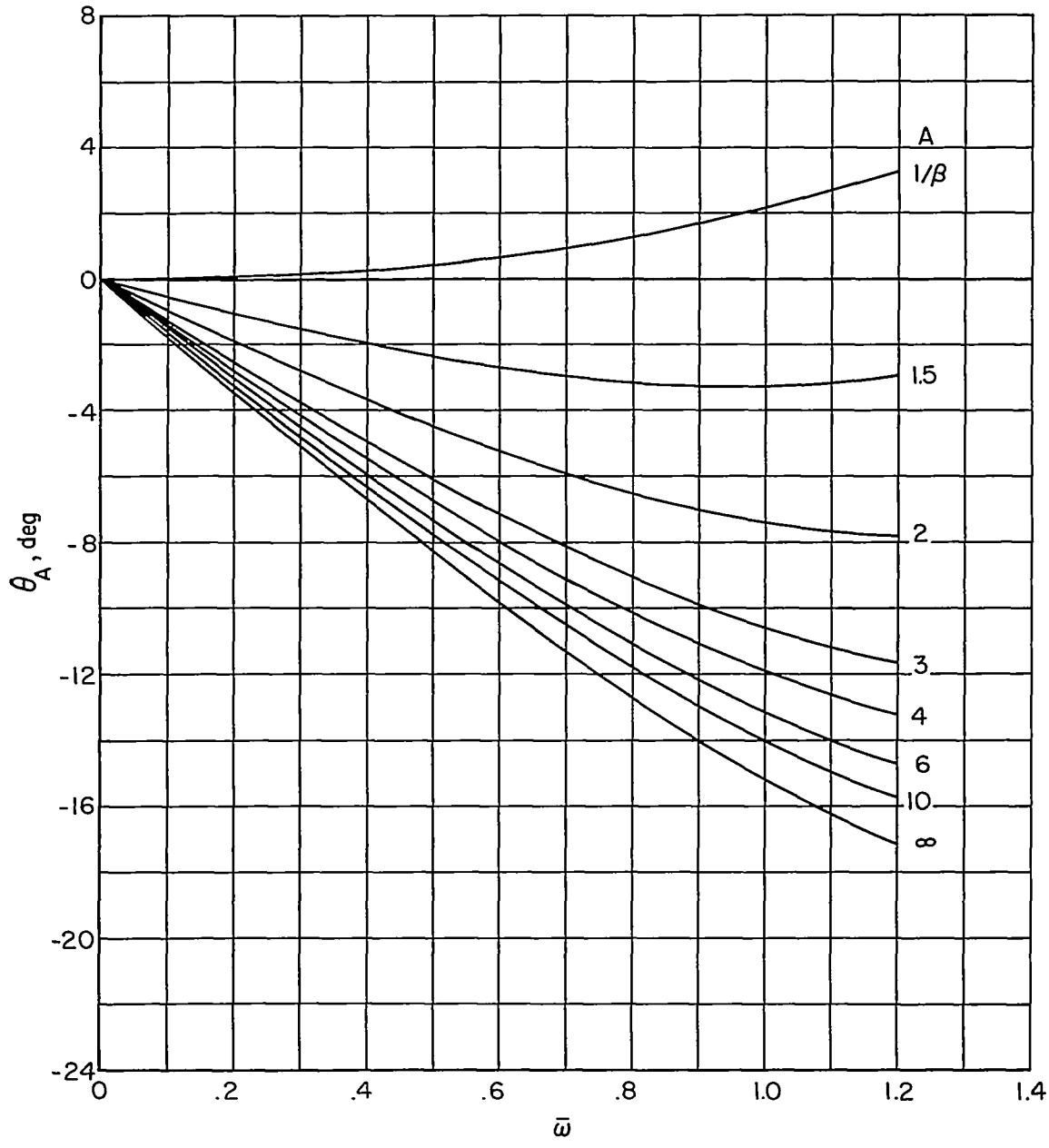

(a) Phase angle between total-lift vector and angular-displacement vector α.

Figure 8.- Phase angles for pitching rectangular wing as functions of $\bar{\omega}$ for $M = 1.3$, $x_o = 0.5$, and various values of A.

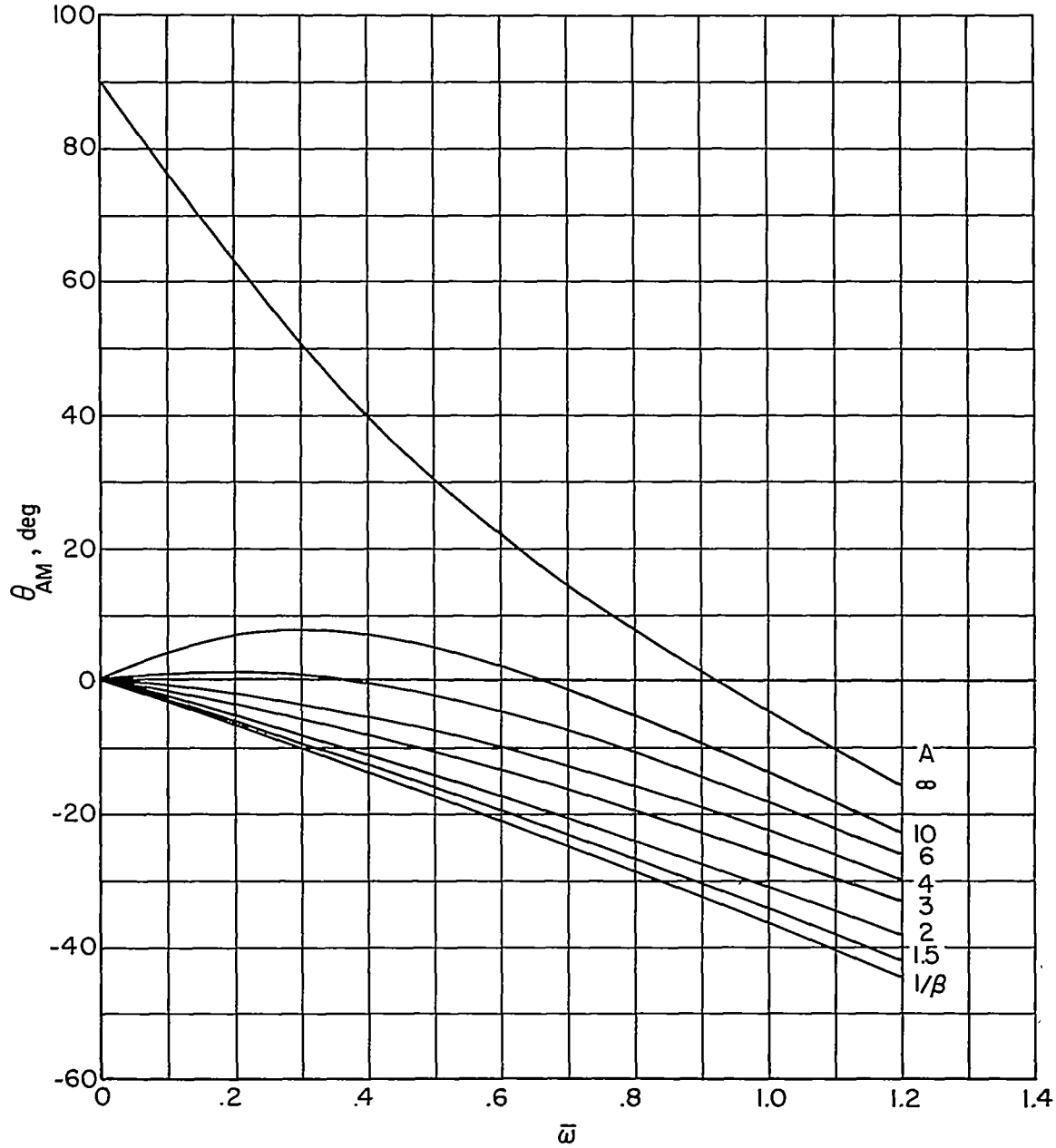

(b) Phase angle between total-moment vector and angular-displacement vector α.

Figure 8.- Concluded.

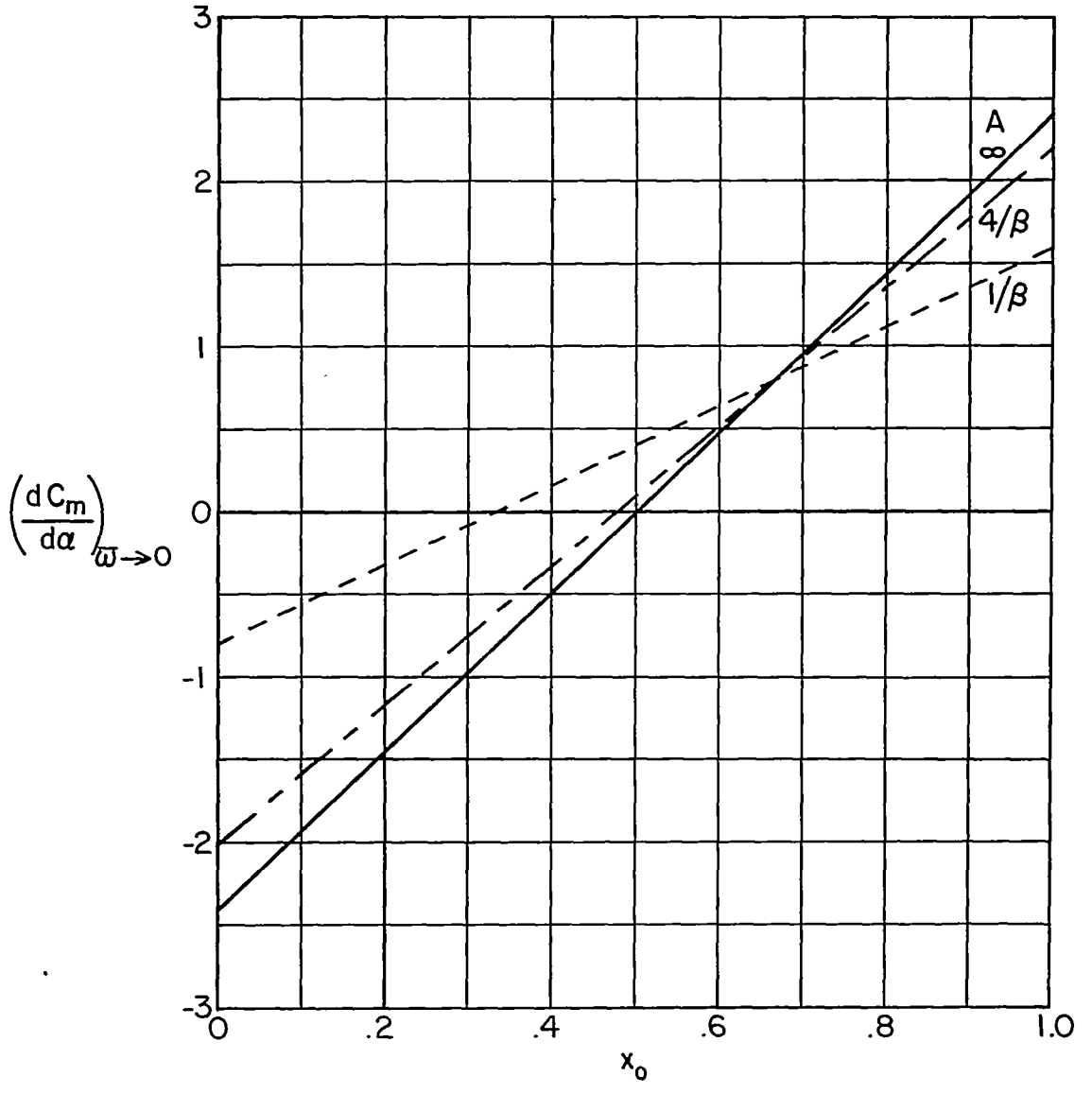

Figure 9.- Total moment-curve slope associated with pitching as a function of x_0 for $M = 1.3$, $\bar{\omega} \longrightarrow 0$, and three values of A.

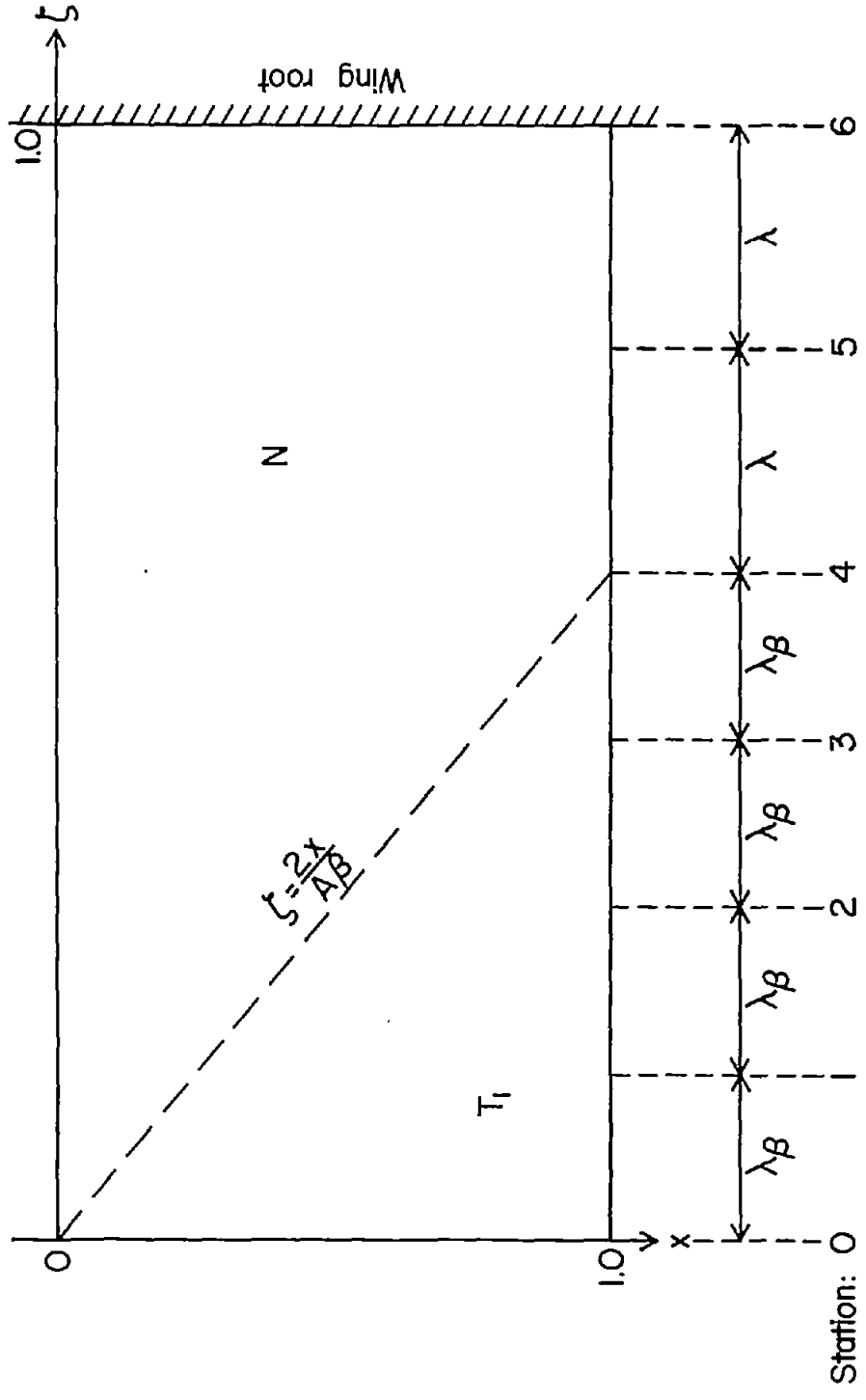

Figure 10.- Sketch illustrating coordinates and stations used in numerical integration method of appendix B.

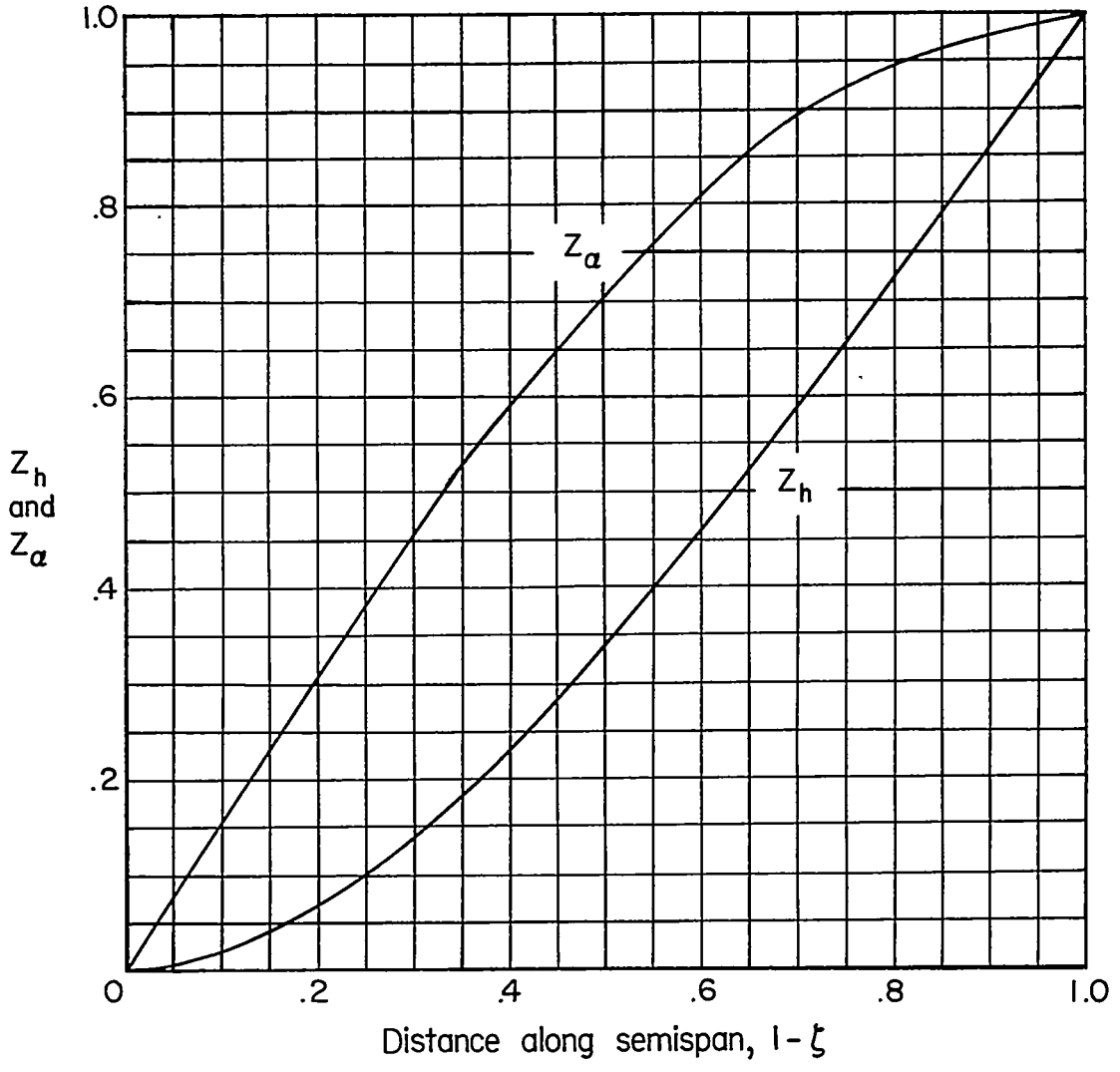

Figure 11.- Uncoupled first bending mode shape Z_h and first torsion mode shape Z_α for a uniform cantilever wing.

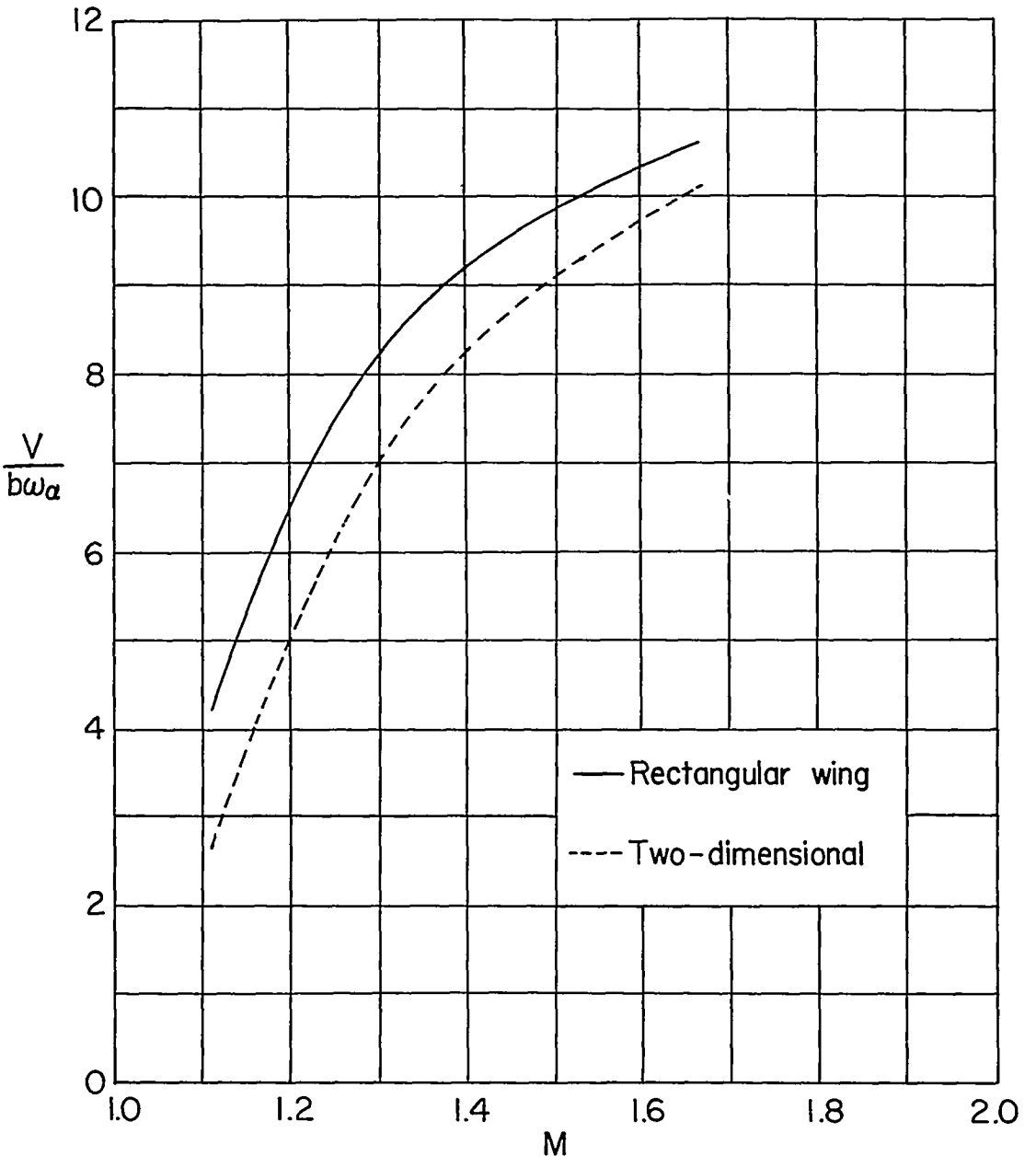

Figure 12.- Flutter-speed coefficients plotted against Mach number calculated from rectangular-wing aerodynamic coefficients and from two-dimensional aerodynamic coefficients for $A = 4.53$, $1/\kappa = 95.3$, $x_o = 0.341$, $x_\alpha = 0.350$, $r_\alpha^2 = 0.39$, and $\omega_h/\omega_\alpha = 0.583$.

NACA-Langley - 4-12-54 - 1000